Západočeská univerzita v Plzni

Fakulta aplikovaných věd

Katedra matematiky

Diplomová práce

Po částech kružnicové spline křivky a jejich aplikace

V Plzni, 2013   **Jana Černá**

University of west Bohemia

Faculty of Applied Sciences

Department of Mathematics

ZÁPADOČESKÁ
UNIVERZITA
V PLZNI

Master thesis

Piecewise circular spline curves and their application

Pilsen, 2013

Jana Černá

Declaration

I do hereby declare that the entire master thesis is my original work and that I have used only the cited sources.

Plzeň, 22. 5. 2013   . . . .

Acknowledgement

Abstrakt

V předkládané diplomové práci jsou studovány po částech kružnicové spline křivky, které jsou utvořeny z biarc křivek. Biarc je křivka složená z dvou oblouků kružnic, které jsou napojeny se zachováním G^1 spojitosti. Hlavním cílem této práce je zkoumat teorii a aplikace biarců v geometrickém modelování a popřípadě některé aplikace vylepšit. Nejprve jsou uvedeny obecné teoretické poznatky o biarc křivkách v rovině a v prostoru. Dále je ukázáno, jak biarc křivkou realizovat Hermitovu interpolaci, tj. jak interpolovat dva body s danými tečnými vektory v těchto bodech. Také je předvedeno, jak popsat biarc jako NURBS křivku. Poté jsou porovnány různé volby napojovacího bodu a vliv této volby na tvar a křivost výsledného biarcu. Dále je ukázána a analyzována aproximace dané křivky se zadanou přesností pomocí biarců. Nakonec jsou realizovány některé aplikace biarců v geometrickém modelování.

Abstract

In this thesis we study piecewise circular spline curves that are formed by biarcs. Biarc is a curve that is entirely composed of two circular arcs joined in a way that G^1 continuity is preserved. The main goal of this thesis is to study the theory and application of biarcs and eventually improve some of the applications in geometric modelling. First, we present general theoretical facts about biarcs in plane and in space. Next, we show how to interpolate set of points with given tangents by biarcs in plane and in space, and thus get Hermite interpolation of the data. We also show how to describe biarc as NURBS curve. Then we compare various choices of joining point and its effect on the shape and curvature of resulting biarc. We also show how to approximate given curve with piecewise circular curve consisted of biarcs when accuracy is given. Finally, we discuss and realize some applications of biarcs in geometrical modelling.

Contents

Introduction

Piecewise circular curve is a curve that consists entirely from circular arcs and straight lines, which can be thought of as arcs with centre at infinity and infinite radius. They are widely used in various industries for example for path planning of a robot, laser or camera. They have also use in Computer Numerical Control (CNC) manufacturing, where it is important to control precisely the speed of the tool along its path. Also, offsets of the curve are used in the CNC machinig, since in many cases some part of the machine must move at a given constant distance from the manufactured shape. This is why piecewise circular curves with simple (analyticaly expressible) arc-length function are very suitable in CNC manufacturing. To form piecewise circular curves we will use biarc curves that are composed of two circular arcs with G^1 continuity preserved at joining point. They were firstly designed for shipbuilding industry in 1970 and provided the basic curve and hull surface definition for the widely-used BRITSHIPS system (see [10]).

In the first chapter, we define biarc and discuss basic properties of biarc in plane and in space. We present theorem that says how to choose a joining point of biarc in order to preserve G^1 continuity. Also, theorem about biarc in $\mathbb{R}^3$ lying on sphere is given. In the second chapter, two constructions of biarc in plane are shown, with one of them extended to space. Theorems about finding centre of circular arc in plane and in space are also given. Third chapter presents construction of biarc in terms of NURBS curve. Formulas for computing control polygon, weight and knot vector are given. In chapter four, we demonstrate four choices of joining point forming so called "equal-chord biarc", "parallel-tangent" biarc, biarc that minimizes difference in curvatures of the two arcs and biarc that is usefull for approximation of curve. In fifth chapter, we show how to approximate curve with biarcs when accuracy is given. Also, example of approximation is shown and order of approximation by "equal-chord" biarcs is derived. In the last sixth chapter, we demonstrate some applications of biarcs in geometric modelling. We show how to use biarcs when approximating intersection of two natural surfaces, intersection of two rational surfaces and when joining canal surfaces.

Chapter 1

Theory of biarc curves

1.1 Biarc in plane

We begin with definition of biarc.

Definition 1.1.1. *The two circular arcs a_1, a_2 are said to form a biarc interpolating given oriented G^1 data, represented by end points $\boldsymbol{P}_1$, $\boldsymbol{P}_2$ and unit tangent vectors $\boldsymbol{t}_1$, $\boldsymbol{t}_2$ if the two circular arcs share one common end point $\boldsymbol{J}$ called joining point and satisfy the following properties:*

1. *The arc a_1 has the end points $\boldsymbol{P}_1$ and $\boldsymbol{J}$, and $\boldsymbol{t}_1$ is tangent to a_1 with orientation corresponding to a parameterization of a_1 from $\boldsymbol{P}_1$ to $\boldsymbol{J}$.*

2. *The arc a_2 has the end points $\boldsymbol{J}$ and $\boldsymbol{P}_2$ and $\boldsymbol{t}_2$ is tangent to a_2 with orientation corresponding to a parameterization of a_2 from $\boldsymbol{J}$ to $\boldsymbol{P}_2$.*

3. *The two arcs have a common unit tangent vector at $\boldsymbol{J}$, with orientation corresponding to a parameterization of a_1 from $\boldsymbol{P}_1$ to $\boldsymbol{J}$ and of a_2 from $\boldsymbol{J}$ to $\boldsymbol{P}_2$.*
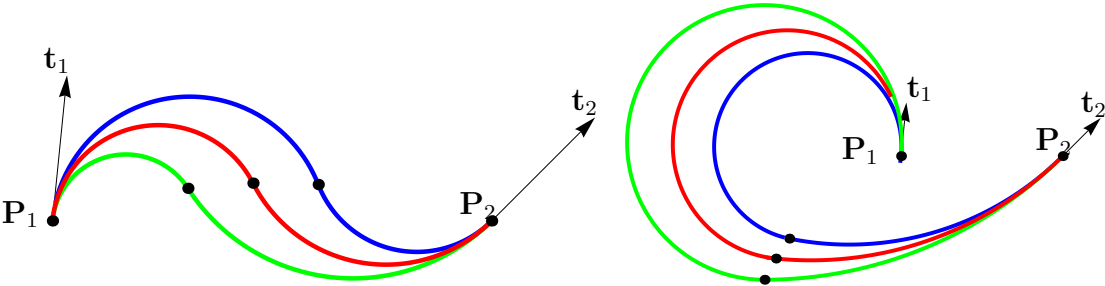

Figure 1.1: Various biarcs for one point-tangent data pair depending on a choice of a joining point. Joining points are shown in black.
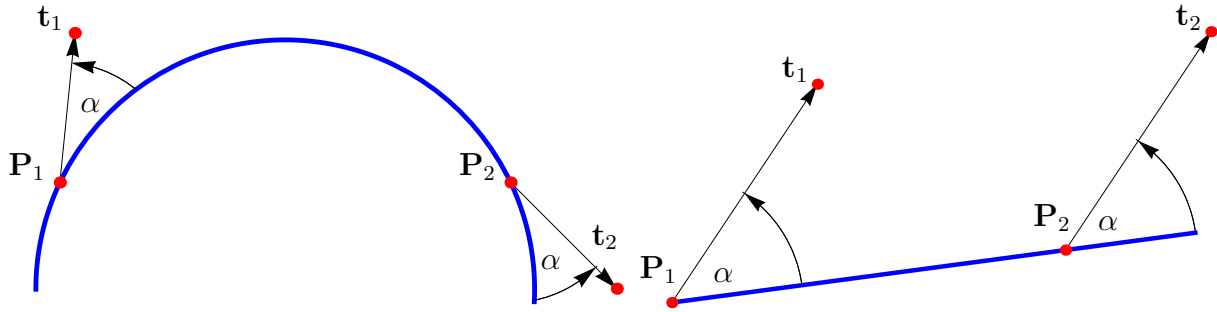
Figure 1.2: Locus of all possible joining points: general case (left) and degenerated case for parallel tangent vectors (right).

We will call the pair $(\mathbf{P}_1, \mathbf{t}_1), (\mathbf{P}_2, \mathbf{t}_2)$ a point-tangent data pair. Definition 1.1.1 provides five conditions. There are in general infinitely many biarcs satisfying these five conditions for one point-tangent data pair. Biarc becomes unique after choice of a joining point $\mathbf{J}$. Following theorem tells us where we should look for this point (c.f. [16]).

Theorem 1.1.1. *The locus of all possible joining points $\boldsymbol{J}$ is the circle l passing through the points $\boldsymbol{P}_1$, $\boldsymbol{P}_2$ and having the same oriented angles with the vectors $\boldsymbol{t}_1$ and $\boldsymbol{t}_2$. If $\boldsymbol{t}_1 = \boldsymbol{t}_2$, then the locus of all possible joining points degeneates into a straight line passing through points $\boldsymbol{P}_1, \boldsymbol{P}_2$.*

Proof of Theorem 1.1.1 can be found in [16]. Next theorem demonstrates how to find the centre and the radius of this circle.

Theorem 1.1.2. *Centre $\boldsymbol{C}$ of locus of all possible joining points can be obtained by intersecting the bisectors of $\boldsymbol{P}_1\boldsymbol{P}_2$ and $\boldsymbol{T}_1\boldsymbol{T}_2$, where $\boldsymbol{T}_1, \boldsymbol{T}_2$ are end points of tangents $\boldsymbol{t}_1, \boldsymbol{t}_2$ shifted to $\boldsymbol{P}_1, \boldsymbol{P}_2$. Radius of the locus is the distance between the centre $\boldsymbol{C}$ and the point $\boldsymbol{P}_1$ or $\boldsymbol{P}_2$, i.e.*

$$r = ||\boldsymbol{C} - \boldsymbol{P}_1|| = ||\boldsymbol{C} - \boldsymbol{P}_2||. \tag{1.1}$$

We can choose joining point $\mathbf{J}$ anywhere on this circle and the final curve will be G^1 continuous (more detailed discussion on how to choose the joining point $\mathbf{J}$ will be given in Chapter 4).

We clasify 2 types of biarcs with respect to their shape. Let us define the unit chord vector between points $\mathbf{P}_1, \mathbf{P}_2$ as

$$\mathbf{e} = \frac{\mathbf{P}_2 - \mathbf{P}_1}{||\mathbf{P}_2 - \mathbf{P}_1||}. \tag{1.2}$$

Next, we denote ϕ_1, ϕ_2 oriented angles that tangent vectors $\mathbf{t}_1, \mathbf{t}_2$ form with the chord vector, respectively.

Definition 1.1.2. *We call the resulting biarc C-shaped, if angles ϕ_1, ϕ_2 have the opposite sign. We call the resulting biarc S-shaped, if angles ϕ_1, ϕ_2 have the same sign or if one of them is 0.*

Note: If both angles ϕ_1, ϕ_2 are zero, then biarc degenerates into a straight line between $\mathbf{P}_1, \mathbf{P}_2$.
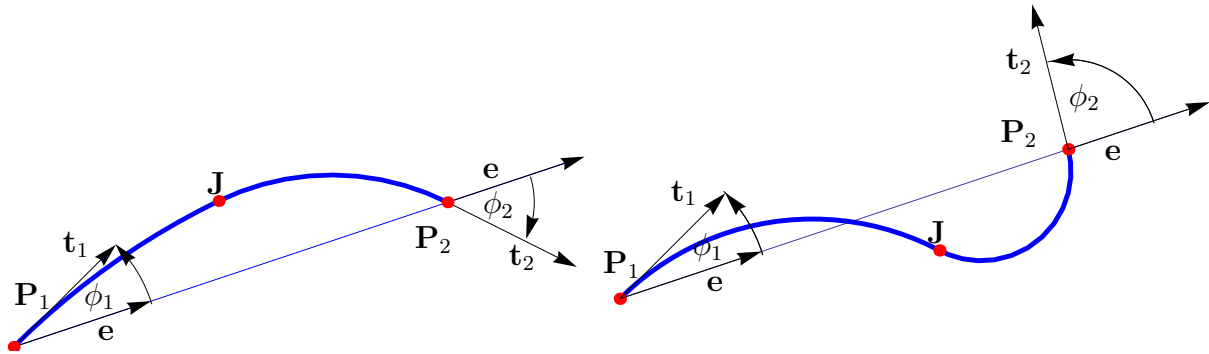
Figure 1.3: C-shaped and S-shaped biarc.

1.2 Biarc in space

In this section we will discuss existence and uniqueness of interpolating biarcs in $\mathbb{R}^3$, but first we need further notation. Given two points $\mathbf{P}_1, \mathbf{P}_2 \in \mathbb{R}^3$, we denote the chord and unit vector along the chord by

$$\mathbf{d} = \mathbf{P}_2 - \mathbf{P}_1, \quad \mathbf{e} = \frac{\mathbf{d}}{||\mathbf{d}||}. \tag{1.3}$$

Theorem 1.2.1. *The rotation matrix that maps a tangent vector $\boldsymbol{t}$ into the (compatibly oriented) vector $\boldsymbol{t}^*$ at $\boldsymbol{P}_1$ of the circle with tangent $\boldsymbol{t}$ at $\boldsymbol{P}_2$ passing through the point $\boldsymbol{P}_1$ is given by*

$$\boldsymbol{R} = 2\boldsymbol{e} \otimes \boldsymbol{e} - \mathbf{I}, \tag{1.4}$$

where $\otimes$ denotes outer product and $\mathbf{I}$ is identity matrix in $\mathbb{R}^3$.

For proof of Theorem 1.2.1, see [15]. Given a point-tangent data pair $(\mathbf{P}_1, \mathbf{t}_1), (\mathbf{P}_2, \mathbf{t}_2)$ we denote

$$\mathbf{t}_2^* = \mathbf{R} \cdot \mathbf{t}_2. \tag{1.5}$$

We clasify four circles

- C_1 – the circle with tangent $\mathbf{t}_1$ at $\mathbf{P}_1$ passing through $\mathbf{P}_2$,

- C_2 – the circle with tangent $\mathbf{t}_2$ at $\mathbf{P}_2$ passing through $\mathbf{P}_1$,

- C_+ – the circle with tangent $\mathbf{t}_1 + \mathbf{t}_2^*$ at $\mathbf{P}_1$ passing through $\mathbf{P}_2$ (if $\mathbf{t}_1 + \mathbf{t}_2^* \neq 0$),

- C_- – the circle with tangent $\mathbf{t}_1 - \mathbf{t}_2^*$ at $\mathbf{P}_1$ passing through $\mathbf{P}_2$ (if $\mathbf{t}_1 - \mathbf{t}_2^* \neq 0$).

We will call a pair of point-tangent data $(\mathbf{P}_1, \mathbf{t}_1), (\mathbf{P}_2, \mathbf{t}_2)$ *cocircular* if $C_1 = C_2$ (i.e., biarc through this data is consisted of one arc). If the data are cocircular, we will call them

- *compatible*, if the orientation of circles C_1, C_2 is the same (and therefore $\mathbf{t}_1 - \mathbf{t}_2^* = 0$ and C_- is not defined),

- *incompatible*, if the orientation of circles C_1, C_2 is opposite (and therefore $\mathbf{t}_1 + \mathbf{t}_2^* = 0$ and C_+ is not defined).
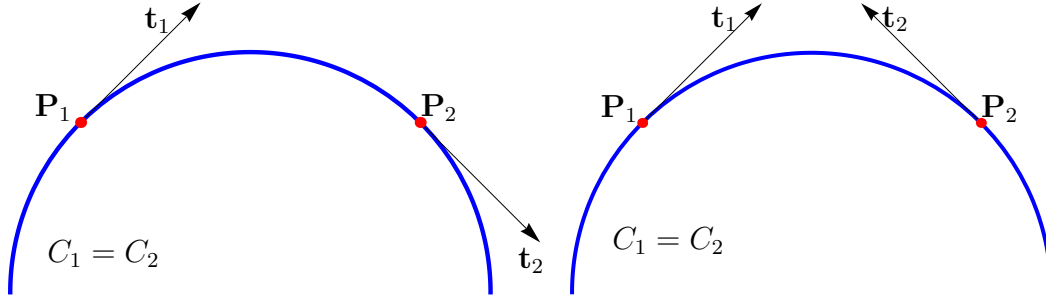
Figure 1.4: Compatible (left) and incompatible (right) data.

Elementary geometry demonstrates that any pair of point-tangent data that are not cocircular define a unique sphere containing both points and with each tangent vector contained in the corresponding tangent plane to the sphere. This sphere generated by $(\mathbf{P}_1, \mathbf{t}_1), (\mathbf{P}_2, \mathbf{t}_2)$, we will denote $\mathbf{S}$. In the case that data $(\mathbf{P}_1, \mathbf{t}_1), (\mathbf{P}_2, \mathbf{t}_2)$ are not cocircular and lie in one plane, i.e. $(\mathbf{t}_1 \times \mathbf{t}_2) \cdot \mathbf{e} = 0$, the sphere $\mathbf{S}$ is a plane that can be considered as a sphere with infinite radius.

Theorem 1.2.2. *When $(\boldsymbol{t}_1 \times \boldsymbol{t}_2) \cdot \boldsymbol{e} \neq 0$, the centre and the radius of the sphere $\boldsymbol{S}$ is given by*

$$\boldsymbol{C} = \boldsymbol{P}_1 + \frac{||\boldsymbol{d}||}{2} \frac{\boldsymbol{t}_2^* \times \boldsymbol{t}_1}{(\boldsymbol{t}_1 \times \boldsymbol{t}_2) \cdot \boldsymbol{e}}, \tag{1.6}$$

$$r = \frac{||\boldsymbol{d}||}{2} \frac{|\sin \alpha|}{|(\boldsymbol{t}_1 \times \boldsymbol{t}_2) \cdot \boldsymbol{e}|} = \frac{||\boldsymbol{d}||}{2} \frac{\sqrt{1 - (\boldsymbol{t}_2^* \cdot \boldsymbol{t}_1)^2}}{|(\boldsymbol{t}_1 \times \boldsymbol{t}_2) \cdot \boldsymbol{e}|}, \tag{1.7}$$

where α is the angle between unit vectors $\boldsymbol{t}_1$ and $\boldsymbol{t}_2^*$.

Proof can be found in [15]. In the non-cocircular case all four circles C_1, C_2, C_+, C_- exist, pass through $\mathbf{P}_1$ and $\mathbf{P}_2$, and lie on the sphere $\mathbf{S}$. The circles C_+ and C_- are mutually perpendicular and bisect the angles between C_1 and C_2 (see Figure 1.5).

We will now discuss uniqueness of interpolating biarc. Let us suppose that $(\mathbf{P}_1, \mathbf{t}_1)$, $(\mathbf{P}_2, \mathbf{t}_2)$ is a non-cocircular point-tangent data pair. How many biarcs are there interpolating this Hermitian data? This question is answered by the crucial theorem of this section (c.f. [15], pp. 41).

Theorem 1.2.3. *For a point-tangent data pair $(\boldsymbol{P}_1, \boldsymbol{t}_1), (\boldsymbol{P}_2, \boldsymbol{t}_2)$ that is non-cocircular (i.e. $C_1 \neq C_2$), there is a nonempty set of possible joining points corresponding to compatibly oriented arcs. For each joining point $\boldsymbol{J}$ the biarc is unique. Moreover*

1. *The locus of all possible joining points is a circle l going through $\boldsymbol{P}_1$ and $\boldsymbol{P}_2$.*

2. *All biarcs lie on the sphere $\boldsymbol{S}$ uniquely determined by $(\boldsymbol{P}_1, \boldsymbol{t}_1), (\boldsymbol{P}_2, \boldsymbol{t}_2)$.*
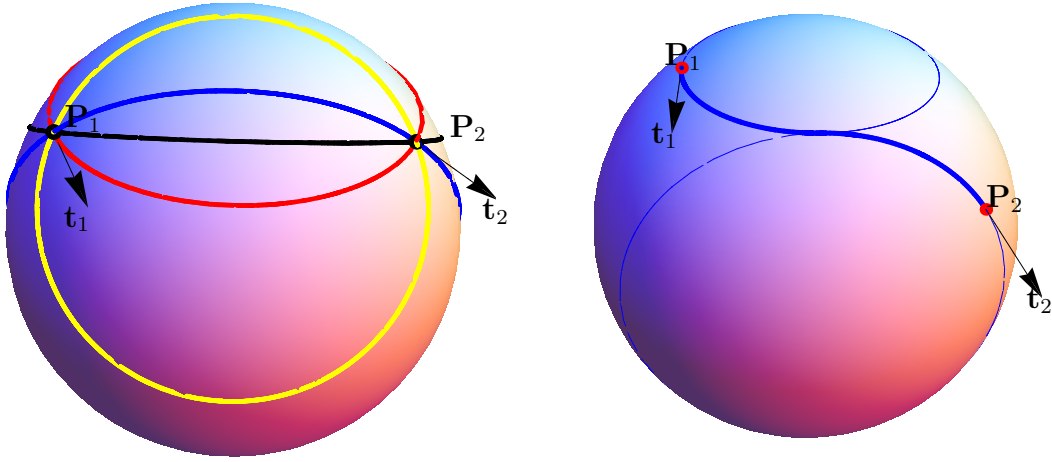
Figure 1.5: Left: Point-tangent data pair and associated circles C_1 (red), C_2 (blue), C_+ (black), C_- (yellow). Right: Biarc and the sphere $\mathbf{S}$.

3. *There is a unique biarc through every point on the sphere $\boldsymbol{S}$ going through $\boldsymbol{P}_1$ and $\boldsymbol{P}_2$ (i.e., the set of all possible biarcs is a simple covering of the sphere $\boldsymbol{S}$).*

One can also show that

- If $(\mathbf{P}_1, \mathbf{t}_1), (\mathbf{P}_2, \mathbf{t}_2)$ is non-cocircular, then l is the circle C_+.

- If $(\mathbf{P}_1, \mathbf{t}_1), (\mathbf{P}_2, \mathbf{t}_2)$ is cocircular, then

  (a) if the data is compatible, l is the common circle $C_+ = C_1 = C_2$,

  (b) if the data is incompatible, l is the sphere $\mathbf{S}$ passing through $\mathbf{P}_1$ and $\mathbf{P}_2$.

- The locus l is a straight line going through $\mathbf{P}_1$ and $\mathbf{P}_2$ if and only if $\mathbf{t}_1 = \mathbf{t}_2$ with $\mathbf{t}_1 \cdot \mathbf{e} \neq 0$.

- The locus l is a plane going through $\mathbf{P}_1$ and $\mathbf{P}_2$ with normal vector $\mathbf{t}_1 \times \mathbf{e}$ if and only if $\mathbf{t}_1 = \mathbf{t}_2$ with $\mathbf{t}_1 \cdot \mathbf{e} = 0$.

Thus, the matching locus of all possible joining points is the circle C_+ whenever it exists, and is otherwise a sphere $\mathbf{S}$. The matching locus l has infinite radius if and only if $\mathbf{t}_1 = \mathbf{t}_2$.

Figure 1.6 shows examples of biarcs for one point-tangent data pair with various choices of joining point $\mathbf{J}$. Note that all biarcs really lie entirely on one sphere $\mathbf{S}$.
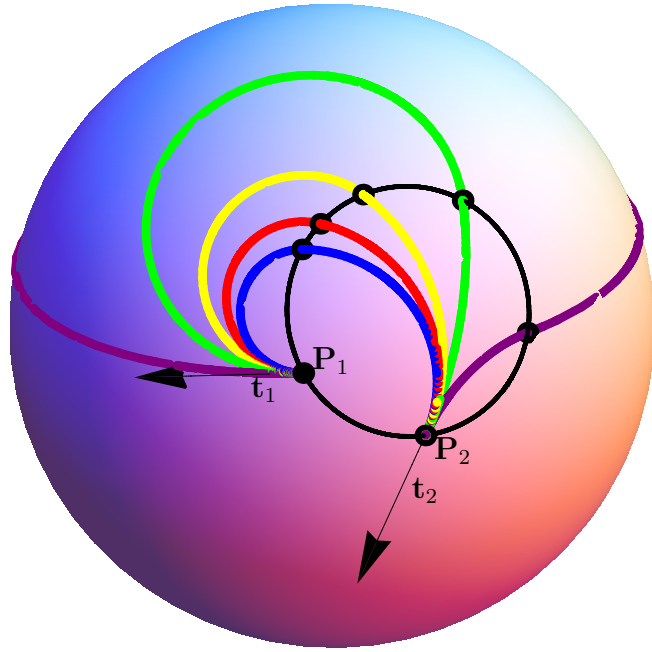
13

Figure 1.6: Several biarcs with different choices of joining point (black points) on the locus of all joining points (black circle).

Chapter 2

Hermite interpolation using biarcs

2.1 Construction of biarc by finding centres of arcs

In this section we show how to obtain centres of arcs that form biarc in plane. Let us suppose we have a point-tangent data pair $(\mathbf{P}_1, \mathbf{t}_1), (\mathbf{P}_2, \mathbf{t}_2)$ we wish to interpolate by a biarc. We choose some joining point $\mathbf{J}$ on the locus of all possible joining points (see Theorem 1.1.1 and 1.1.2).

Next theorem shows how to find centre and radius of the circle interpolating data $\mathbf{A}, \mathbf{B}, \mathbf{t} \in \mathbb{R}^2$, i.e. the circle that goes from $\mathbf{A}$ to $\mathbf{B}$ and has unit tangent vector $\mathbf{t}$ at $\mathbf{A}$.

Theorem 2.1.1. *Centre $\boldsymbol{C}$ of the interpolating circle from $\boldsymbol{A}$ to $\boldsymbol{B}$ with unit tangent vector $\boldsymbol{t}$ at $\boldsymbol{A}$ can be found as*

$$\boldsymbol{C} = \boldsymbol{V} + \frac{||\boldsymbol{B} - \boldsymbol{A}||}{2\tan\alpha}\boldsymbol{n}, \tag{2.1}$$

where $\boldsymbol{V} = \dfrac{\boldsymbol{A} + \boldsymbol{B}}{2}$, $\alpha = \arccos\left(\boldsymbol{e} \cdot \boldsymbol{t}\right)$ and $\boldsymbol{n}$ is vector perpendicular to unit chord vector $\boldsymbol{e}$ (see Figure 2.1).

For proof see [4]. Radius of the circle can be again obtained as the distance between the centre and some point on the circle

$$r = ||\mathbf{C} - \mathbf{A}||. \tag{2.2}$$

The well known parametric equation of a circle with centre $\mathbf{C} = [x_\mathbf{C}, y_\mathbf{C}]$ and radius r can be written as

$$x = x_\mathbf{C} + r\cos t, \tag{2.3}$$

$$y = y_\mathbf{C} + r\sin t, \tag{2.4}$$

where $t \in \langle 0, 2\pi \rangle$. By the above description we find centres and radii of two circles interpolating a point-tangent data pair $(\mathbf{P}_1, \mathbf{t}_1), (\mathbf{P}_2, \mathbf{t}_2)$. Next, we need to find desired parts of each circle to form biarc. We need to find parameter interval $\langle t_S, t_E \rangle$, where t_S is start
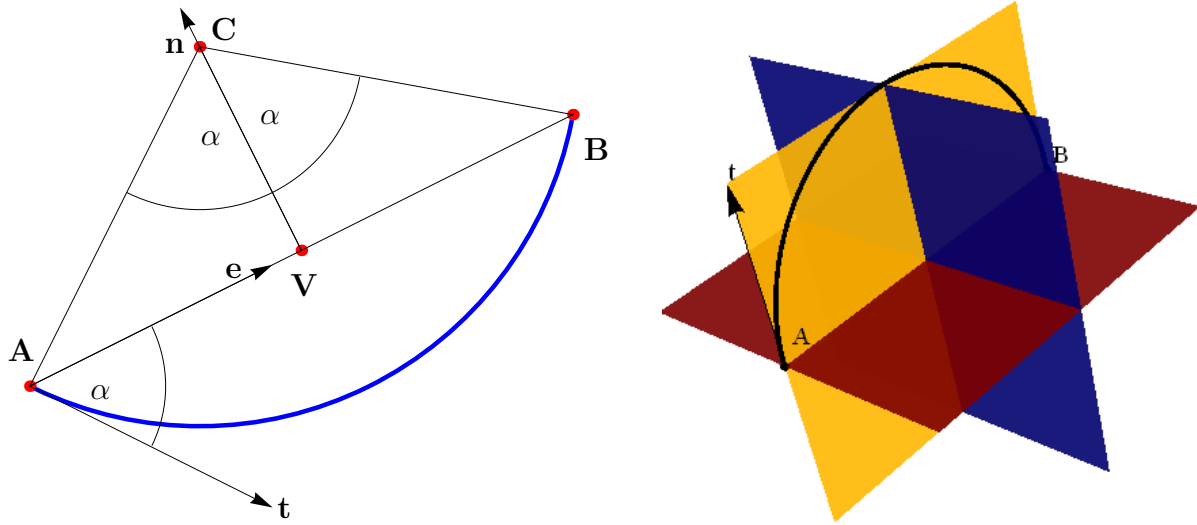
Figure 2.1: Finding centre of interpolating circle in $\mathbb{R}^2$ (left) and in $\mathbb{R}^3$ (right).

parameter value and t_E is end parameter value. We denote $\mathbf{A} = [x_{\mathbf{A}}, y_{\mathbf{A}}], \mathbf{B} = [x_{\mathbf{B}}, y_{\mathbf{B}}]$.
Solving system

$$x_{\mathbf{A}} = x_{\mathbf{C}} + r\cos t, \tag{2.5}$$

$$y_{\mathbf{A}} = y_{\mathbf{C}} + r\sin t, \tag{2.6}$$

gives start value t_S and solving system

$$x_{\mathbf{B}} = x_{\mathbf{C}} + r\cos t, \tag{2.7}$$

$$y_{\mathbf{B}} = y_{\mathbf{C}} + r\sin t. \tag{2.8}$$

gives end value t_E. Equations (2.3) and (2.4) with $t \in \langle t_S, t_E \rangle$ describe a circular arc from $\mathbf{A}$ to $\mathbf{B}$ with centre at $\mathbf{C}$ and radius r.

Figure 2.2 shows biarc that was constructed by this method for data

$$\mathbf{P_1} = [0,0], \ \mathbf{P_2} = [3, 0.5], \ \mathbf{t_1} = (0,1), \ \mathbf{t_2} = \frac{1}{\sqrt{5}}(1,2), \tag{2.9}$$

where the first arc is described by

$$x(t) = 0.796745 + 0.796745\cos t,$$
$$y(t) = 0.796745\sin t,$$
$$t \in \langle 0.562121, 3.14159 \rangle$$

and second arc by

$$x(t) = 2.21423 + 0.878518\cos t,$$
$$y(t) = 0.892885 + 0.878518\sin t,$$
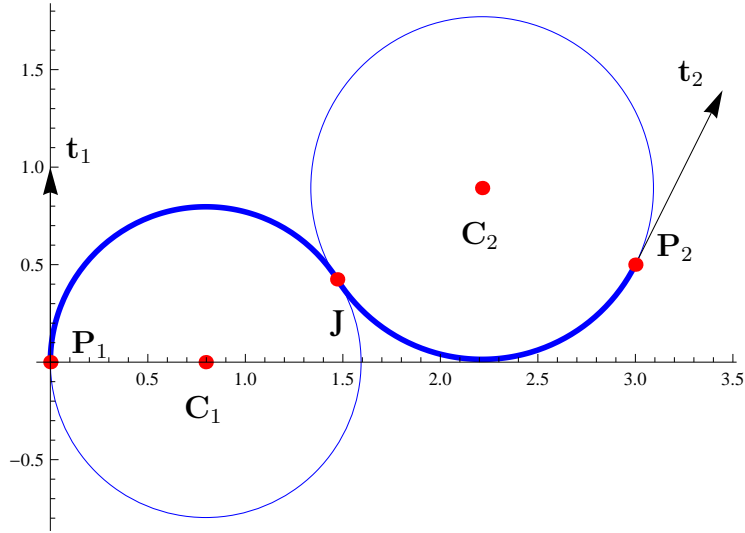$$t \in \langle 3.70372, 5.81954 \rangle.$$

16

Figure 2.2: Biarc constructed by finding centres of arcs.

Similar method can be used in $\mathbb{R}^3$. Next theorem says how to find centre of arc through points $\mathbf{A}, \mathbf{B}$ with unit tangent vector $\mathbf{t}$ at $\mathbf{A}$ in $\mathbb{R}^3$.

Theorem 2.1.2. *Centre $\boldsymbol{C}$ of arc through data $\boldsymbol{A}, \boldsymbol{B}, \boldsymbol{t} \in \mathbb{R}^3$ can be found as an intersection of three planes $\boldsymbol{S}_1, \boldsymbol{S}_2, \boldsymbol{S}_3$, where*

- $\boldsymbol{S}_1$ *is a plane that contains point $\boldsymbol{A}$ and $\boldsymbol{t}$ is its normal vector,*

- $\boldsymbol{S}_2$ *is a plane that contains point $\dfrac{\boldsymbol{A} + \boldsymbol{B}}{2}$ and chord vector $\boldsymbol{e} = \dfrac{\boldsymbol{B} - \boldsymbol{A}}{||\boldsymbol{B} - \boldsymbol{A}||}$ is its normal vector,*

- $\boldsymbol{S}_3$ *is a plane that contains biarc, i.e. plane that contains $\boldsymbol{A}$ and its normal vector is $\boldsymbol{t} \times \boldsymbol{e}$.*

Radius is again given by $r = ||\mathbf{A} - \mathbf{C}||$. Next, we would have to find two perpendicular vectors in the plane that the circle lies in and then find parameter interval $\langle t_S, t_E \rangle$ to form arc. However, it is unnecessarily complicated procedure and there is better way how to construct an arc in plane and in space as we will see in the next section. Nevertheless, Theorem 2.1.2 will become useful in Chapter 5 when we will need centres of arcs to measure a distance of biarc from a curve.

2.2 Construction of biarc by rotating chord vector

In this section we will show how to construct arc through points $\mathbf{A}$ and $\mathbf{B}$ with tangent $\mathbf{t}$ at $\mathbf{A}$ by rotating the the unit chord vector between points $\mathbf{A}$ and $\mathbf{B}$. Let us have a unit chord vector

$$\mathbf{e} = \frac{\mathbf{B} - \mathbf{A}}{||\mathbf{B} - \mathbf{A}||}. \tag{2.10}$$
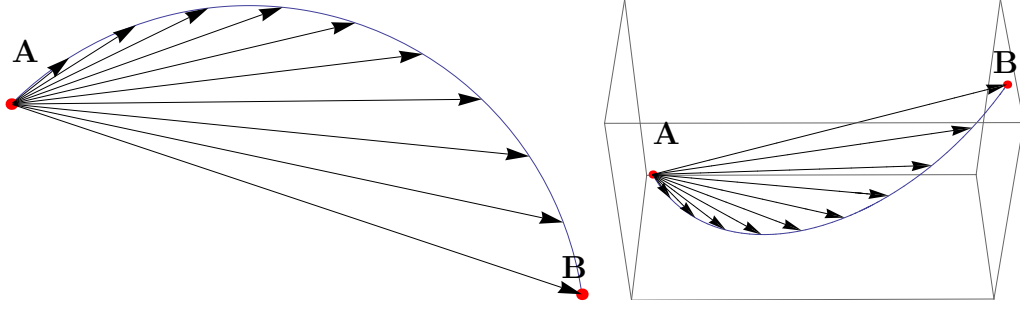
17

Figure 2.3: Construction of arc by rotating chord vector

Algorithm 1 $getArc(\mathbf{A}, \mathbf{B}, \mathbf{t})$	**Algorithm 2** $getArc3D(\mathbf{A}, \mathbf{B}, \mathbf{t})$
1: $\mathbf{e} = \dfrac{\mathbf{B} - \mathbf{A}}{\lvert\lvert\mathbf{B} - \mathbf{A}\rvert\rvert}$	1: $\mathbf{e} = \dfrac{\mathbf{B} - \mathbf{A}}{\lvert\lvert\mathbf{B} - \mathbf{A}\rvert\rvert}$
2: $\alpha = \arccos(\mathbf{e} \cdot \mathbf{t})$	2: $\alpha = \arccos(\mathbf{e} \cdot \mathbf{t})$
3: $\varphi(u) = (u - 1)\alpha$	3: $\varphi(u) = (u - 1)\alpha$
4: $\delta(u) = \lvert\lvert\mathbf{B} - \mathbf{A}\rvert\rvert\dfrac{\sin(u\alpha)}{\sin\alpha}$	4: $\delta(u) = \lvert\lvert\mathbf{B} - \mathbf{A}\rvert\rvert\dfrac{\sin(u\alpha)}{\sin\alpha}$
5: $\mathbf{a}(u) = \mathbf{A} + \begin{pmatrix} \cos\varphi(u) & -\sin\varphi(u) \\ \sin\varphi(u) & \cos\varphi(u) \end{pmatrix} \cdot (\delta\mathbf{e})$	5: $\mathbf{a}(u) = \mathbf{A} + \mathbf{R}(\varphi, \mathbf{t}, \mathbf{e}) \cdot (\delta\mathbf{e})$
Return: $\mathbf{a}(u)$	**Return**: $\mathbf{a}(u)$

We denote α the angle between the unit chord vector $\mathbf{e}$ and the tangent vector $\mathbf{t}$, i.e.,

$$\alpha = \arccos(\mathbf{e} \cdot \mathbf{t}). \tag{2.11}$$

Next, we define angle and distance parametrizations (c.f. [12])

$$\varphi(u) = (u - 1)\alpha, \ u \in \langle 0, 1 \rangle, \tag{2.12}$$

$$\delta(u) = \lvert\lvert\mathbf{B} - \mathbf{A}\rvert\rvert\frac{\sin(u\alpha)}{\sin\alpha}, \ u \in \langle 0, 1 \rangle. \tag{2.13}$$

Now, we can form arc $\mathbf{a}(u)$ by rotating the unit chord vector $\mathbf{e}$ by parametrized angle $\varphi(u)$ and multiplied by the parametrized distance $\delta(u)$ (see Figure 2.3). The above procedure can be written as Algorithm 1: $getArc(\mathbf{A}, \mathbf{B}, \mathbf{t})$. The same procedure can also be applied to construct an arc in $\mathbb{R}^3$ space. But in this case, we need to specify the plane in which we rotate. It is the plane spanned by $\mathbf{t}$ and $\mathbf{e}$. The Algorithm 2: $getArc3D(\mathbf{A}, \mathbf{B}, \mathbf{t})$ shows construction in $\mathbb{R}^3$ space.[1]

Advantage of this construction is that the arc $\mathbf{a}(u)$ for $u \in \langle 0, 1 \rangle$ automatically starts at $\mathbf{A}$ and ends at $\mathbf{B}$. Disadvantage of this construction is that the parametric description

---

[1]The form of rotation matrix in $\mathbb{R}^3$ is complicated, so in Algorithm 2 we use the notation $R(\varphi, \mathbf{t}, \mathbf{e})$ meaning rotation by angle φ in plane spanned by $\mathbf{t}$ and $\mathbf{e}$.

is more complicated – it contains sine and cosine multiples.

We can also obtain locus of all possible joining points for data $(\mathbf{P}_1, \mathbf{t}_1), (\mathbf{P}_2, \mathbf{t}_2)$ by Algorithm 1 and Algorithm 2. First, we need to find a tangent vector $\mathbf{t}_L$ of the locus at point $\mathbf{P}_1$ (so far we only know that locus has the same angle with $\mathbf{t}_1$ and $\mathbf{t}_2$). We recall the definition of a rotation matrix that maps a tangent vector $\mathbf{t}$ at $\mathbf{P}_2$ into the (compatibly oriented) vector $\mathbf{t}^*$ at $\mathbf{P}_1$ of the circle with tangent $\mathbf{t}$ at $\mathbf{P}_2$ passing through the point $\mathbf{P}_1$, i.e.,

$$\mathbf{R} = 2\mathbf{e} \otimes \mathbf{e} - \mathbf{I}, \tag{2.14}$$

where $\mathbf{I}$ is identity matrix. Then the tangent vector $\mathbf{t}_L$ of the locus circle at $\mathbf{P}_1$ can be obtained as

$$\mathbf{t}_L = \mathbf{t}_1 + \mathbf{t}_2^*, \tag{2.15}$$

where $\mathbf{t}_2^*$ is vector obtained by

$$\mathbf{t}_2^* = \mathbf{R} \cdot \mathbf{t}_2. \tag{2.16}$$

Now we can construct locus by $\text{getArc}(\mathbf{P}_1, \mathbf{P}_2, \mathbf{t}_L)$ in plane and by $\text{getArc3D}(\mathbf{P}_1, \mathbf{P}_2, \mathbf{t}_L)$ in space. Actually, for $u \in \langle 0, 1 \rangle$ we do not get the whole locus circle but only arc of the locus, that starts at $\mathbf{P}_1$ and ends at $\mathbf{P}_2$. But this is not a problem because we will usually choose joining point on this arc, since joining points chosen outside of this arc form unnecesarily long biarcs. In the middle of this locus arc (i.e. for $u = 0.5$) we get a joining point $\mathbf{J}$ that has the same distance to $\mathbf{P}_1$ as to $\mathbf{P}_2$ and we can form so called "equal-chord" biarc (discussion about how to choose a joining point will be given in Chapter 4).

When we have constructed locus arc to get a joining point $\mathbf{J}$, we construct two arcs $\mathbf{a}_1(u)$, $\mathbf{a}_2(u)$ that form biarc by

$$\mathbf{a}_1(u) = \text{getArc}(\mathbf{P}_1, \mathbf{J}, \mathbf{t}_1), \ \ \mathbf{a}_2(u) = \text{getArc}(\mathbf{P}_2, \mathbf{J}, -\mathbf{t}_2). \tag{2.17}$$

Notice that arc $\mathbf{a}_2(u)$ will be oriented from $\mathbf{P}_2$ to $\mathbf{J}$, which is opposite orientation than we want. However, in one step we can fix this and join the two arc in one by forming reparametrized piecewise function

$$\mathbf{b}(t) = \begin{cases} \mathbf{a}_1(t) & \text{if } t \leq \frac{1}{2}, \text{where } t = \dfrac{u}{2} \\ \mathbf{a}_2(t) & \text{if } t > \dfrac{1}{2}, \text{where } t = 1 - \dfrac{u}{2} \end{cases} \tag{2.18}$$

where $t \in \langle 0, 1 \rangle$. Equation (2.18) is equation of biarc that gives values of $\mathbf{P}_1$ for $t = 0$, $\mathbf{J}$ for $t = \dfrac{1}{2}$ and $\mathbf{P}_2$ for $t = 1$.

Figure 2.4 shows biarc for data (2.9) constructed by this method, where the first arc $\mathbf{a}_1(t)$ for $t \in \langle 0, 0.5 \rangle$ has equation

$x(t) = 1.59349 \sin{(2.57947t)}[0.960762 \cos{(1.28974(1 - 2t))} - 0.277375 \sin{(1.28974(1 - 2t))}],$
$y(t) = 1.59349 \sin{(2.57947t)}[0.277375 \cos{(1.28974(1 - 2t))} + 0.960762 \sin{(1.28974(1 - 2t))}]$
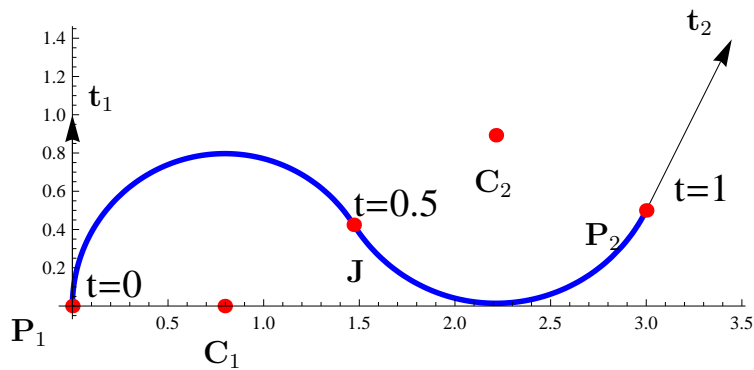
Figure 2.4: Biarc constructed by rotating the chord vector. Notice the parameter values at $\mathbf{P}_1, \mathbf{J}$ and $\mathbf{P}_2$.

and the second arc $\mathbf{a}_2(t)$ for $t \in \langle 0.5, 1 \rangle$ has equation

$$
\begin{aligned}
x(t) &= 3 + 1.75704 \sin\left(2.11582(1-t)\right)[-0.998788 \cos\left(1.05791 - 2.11582(1-t)\right)+ \\
&\quad + 0.0492169 \sin\left(1.05791 - 2.11582(1-t)\right)], \\
y(t) &= 0.5 + 1.75704 \sin\left(2.11582(1-t)\right)[-0.0492169 \cos\left(1.05791 - 2.11582(1-t)\right)- \\
&\quad - 0.998788 \sin\left(1.05791 - 2.11582(1-t)\right)].
\end{aligned}
$$

If we wish to interpolate more than two points (with two tangents) we can split given data to point-tangent data pairs

$$(\mathbf{P}_1, \mathbf{t}_1), (\mathbf{P}_2, \mathbf{t}_2),$$

$$(\mathbf{P}_2, \mathbf{t}_2), (\mathbf{P}_3, \mathbf{t}_3),$$

$$...$$

$$(\mathbf{P}_i, \mathbf{t}_i), (\mathbf{P}_j, \mathbf{t}_j),$$

and use the above mentioned procedure for each pair. Example of such a curve can be seen in Figure 2.5.
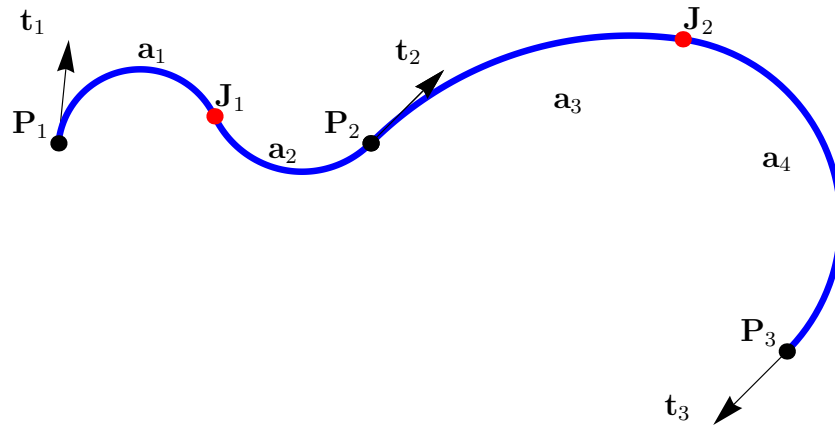
Figure 2.5: Piecewise circular spline curve consisted of two biarcs.

Chapter 3

Biarc as NURBS

3.1   Control polygon, knots and weights

In this section we will derive very efficient way how to describe biarc by NURBS formulation. For more information about NURBS, see for example [8]. We start by determining control points. We need three control points for each of the two arcs, whereas one point (joining point) will be common. So generally we need to determine 5 control points. We set $\mathbf{P}_1$ and $\mathbf{P}_2$ to be start and end point of the control polygon, respectively. We denote three remaining unknown points $\mathbf{A}_1, \mathbf{J}, \mathbf{A}_2$. We want the first arc to start at $\mathbf{P}_1$ and have unit tangent vector $\mathbf{t}_1$ at $\mathbf{P}_1$ and we want the second arc to end at point $\mathbf{P}_2$ and have unit tangent vector $\mathbf{t}_2$ at $\mathbf{P}_2$. Thus, it holds

$$\mathbf{A}_1 = \mathbf{P}_1 + \alpha \mathbf{t}_1, \tag{3.1}$$

$$\mathbf{A}_2 = \mathbf{P}_2 - \beta \mathbf{t}_2, \tag{3.2}$$

where α, β are for now unknown positive numbers such that α is the distance of $\mathbf{A}_1$ from $\mathbf{P}_1$ and β is the distance of $\mathbf{A}_2$ from $\mathbf{P}_2$. Now we determine the point $\mathbf{J}$, that should lie on the abscisse between $\mathbf{A}_1, \mathbf{A}_2$, in order to get G^1 continuity at the point $\mathbf{J}$. There are many ways how to choose the ratio γ of the distance of this point from $\mathbf{A}_1$ and from $\mathbf{A}_2$, i.e.

$$\gamma = \frac{|\mathbf{A}_1 \mathbf{J}|}{|\mathbf{A}_2 \mathbf{J}|} = \frac{\alpha}{\beta}. \tag{3.3}$$

Choice of this ratio corresponds to choice of a joining point. Since the control triangle of circular arc must be an isosceles triangle and with respect to (3.1), (3.2), we get

$$|\mathbf{A}_1 \mathbf{J}| = |\mathbf{A}_1 \mathbf{P}_1| = \alpha, \tag{3.4}$$

$$|\mathbf{A}_2 \mathbf{J}| = |\mathbf{A}_2 \mathbf{P}_2| = \beta. \tag{3.5}$$

We can rewrite above equations as

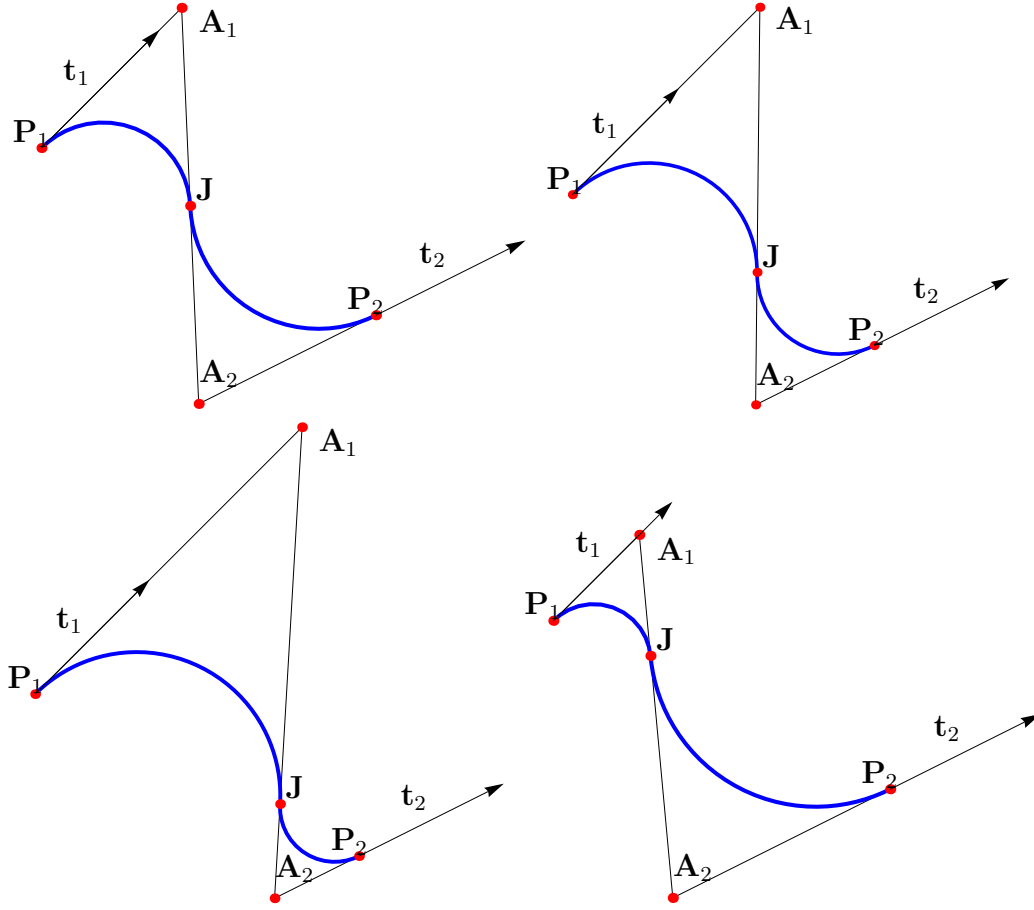$$(\mathbf{A}_1 - \mathbf{J}).(\mathbf{A}_1 - \mathbf{J}) = \alpha^2, \tag{3.6}$$

Figure 3.1: Interpolation of one point-tangent data pair by NURBS biarc with ratio $\frac{\alpha}{\beta} = 1, 2, 4, 0.25$ respectively

$$(\mathbf{J} - \mathbf{A}_2).(\mathbf{J} - \mathbf{A}_2) = \beta^2. \tag{3.7}$$

So we are looking for a joining point for which

$$\mathbf{J} = \frac{\beta}{\alpha + \beta}\mathbf{A}_1 + \frac{\alpha}{\alpha + \beta}\mathbf{A}_2. \tag{3.8}$$

By substituting (3.1) and (3.2) to (3.8) one gets

$$\mathbf{J} = \frac{\beta}{\alpha + \beta}(\mathbf{P}_1 + \alpha\mathbf{t}_1) + \frac{\alpha}{\alpha + \beta}(\mathbf{P}_2 - \beta\mathbf{t}_2).$$

We take $\frac{\alpha}{\alpha + \beta}$ in front of the expression on the right and the above equation becomes

$$\mathbf{J} = \frac{\alpha}{\alpha + \beta}\left[\frac{\beta}{\alpha}\mathbf{P}_1 + \beta\mathbf{t}_1 + \mathbf{P}_2 - \beta\mathbf{t}_2\right]. \tag{3.9}$$

Now we use (3.9) to express the difference vectors $\mathbf{A}_1 - \mathbf{J}$ and $\mathbf{J} - \mathbf{A}_2$

$$\mathbf{A}_1 - \mathbf{J} = \mathbf{P}_1 + \alpha\mathbf{t}_1 - \frac{\alpha}{\alpha+\beta}\left[\frac{\beta}{\alpha}\mathbf{P}_1 + \beta\mathbf{t}_1 + \mathbf{P}_2 - \beta\mathbf{t}_2\right]$$

$$= \frac{\alpha}{\alpha+\beta}\left[\frac{\alpha+\beta}{\alpha}\mathbf{P}_1 + (\alpha+\beta)\mathbf{t}_1 - \frac{\beta}{\alpha}\mathbf{P}_1 - \beta\mathbf{t}_1 - \mathbf{P}_2 + \beta\mathbf{t}_2\right]$$

$$= \frac{\alpha}{\alpha+\beta}\left[\mathbf{P}_1 - \mathbf{P}_2 + \alpha\mathbf{t}_1 + \beta\mathbf{t}_2\right].$$

We denote $\mathbf{d} = \mathbf{P}_2 - \mathbf{P}_1$ and we can write

$$\mathbf{A}_1 - \mathbf{J} = \frac{\alpha}{\alpha+\beta}\left[-\mathbf{d} + \alpha\mathbf{t}_1 + \beta\mathbf{t}_2\right]. \tag{3.10}$$

We insert (3.10) to (3.6) and get

$$(\mathbf{A}_1 - \mathbf{J})^2 - \alpha^2 = \frac{\alpha^2}{(\alpha+\beta)^2}\left[-\mathbf{d} + \alpha\mathbf{t}_1 + \beta\mathbf{t}_2\right]^2 - \alpha^2 =$$

$$= \frac{\alpha^2}{(\alpha+\beta)^2}\left[\mathbf{d}^2 + \alpha^2\mathbf{t}_1^2 + \beta^2\mathbf{t}_2^2 - 2\alpha\mathbf{d}\cdot\mathbf{t}_1 + 2\alpha\beta\mathbf{t}_1\cdot\mathbf{t}_2 - 2\beta\mathbf{d}\cdot\mathbf{t}_2\right] = 0$$

and since $\mathbf{t}_1$ and $\mathbf{t}_2$ are unit vectors

$$\frac{\alpha^2}{(\alpha+\beta)^2}\left[\mathbf{d}^2 + \alpha^2 + \beta^2 - 2\alpha\mathbf{d}\cdot\mathbf{t}_1 + 2\alpha\beta\mathbf{t}_1\cdot\mathbf{t}_2 - 2\beta\mathbf{d}\cdot\mathbf{t}_2\right] = 0. \tag{3.11}$$

We multiply equation (3.11) by $\frac{(\alpha+\beta)^2}{\alpha^2}$ and get (c.f. [7])

$$\mathbf{d}^2 - 2\alpha\mathbf{d}\cdot\mathbf{t}_1 - 2\beta\mathbf{d}\cdot\mathbf{t}_2 + 2\alpha\beta(\mathbf{t}_1\cdot\mathbf{t}_2 - 1) = 0. \tag{3.12}$$

This equation has unknowns only α and β. When the value of ratio $\frac{\alpha}{\beta}$ is set, (3.12) is ordinary quadratic equation with unknown α. We solve it and choose the positive root. Next, we plug α and β to (3.1),(3.2),(3.8) and the control polygon is determined. To form a NURBS curve, knot values are also needed. Let us define knot vector as (see [7])

$$K = \{0, 0, 0, T, T, 1, 1, 1\}, \tag{3.13}$$

where

$$T = \frac{|\mathbf{P}_1\mathbf{J}|}{|\mathbf{P}_1\mathbf{J}| + |\mathbf{J}\mathbf{P}_2|}. \tag{3.14}$$

Also, weights of control points need to be set. It is well known, that in order to produce a circular arc from a curve with three control points, the end points must have a unitary weight, while the weight of the central control point must be equal to the cosine of half the angle between the segments joining the points. So the weight vector for biarc has a form

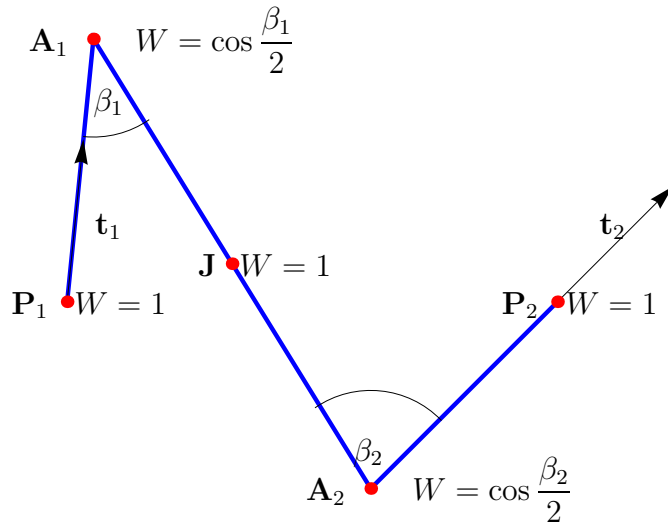$$W = \left\{1, \cos\frac{\beta_1}{2}, 1, \cos\frac{\beta_2}{2}, 1\right\}, \tag{3.15}$$

Figure 3.2: Control polygon

where β_1 is the angle between $\mathbf{P}_1, \mathbf{A}_1$ and $\mathbf{J}, \mathbf{A}_1$, and β_2 is the angle between $\mathbf{J}, \mathbf{A}_2$ and $\mathbf{P}_2, \mathbf{A}_2$ (see Figure 3.2).

Finally, we can construct biarc as a NURBS curve with control polygon $\{\mathbf{P}_1, \mathbf{A}_1, \mathbf{J}, \mathbf{A}_2, \mathbf{P}_2\}$, knot vector K and weight vector W.

3.2 NURBS biarc with $\alpha = \beta$

If we set $\alpha = \beta$, we get control polygon such that

$$\frac{\alpha}{\beta} = \frac{|\mathbf{P}_1\mathbf{A}_1|}{|\mathbf{P}_2\mathbf{A}_2|} = \frac{|\mathbf{A}_1\mathbf{J}|}{|\mathbf{A}_2\mathbf{J}|} = 1. \tag{3.16}$$

It makes computations simpler, because (3.12) reduces to

$$\mathbf{d} \cdot \mathbf{d} - 2\alpha\mathbf{d} \cdot (\mathbf{t}_1 + \mathbf{t}_2) + 2\alpha^2(\mathbf{t}_1 \cdot \mathbf{t}_2 - 1) = 0. \tag{3.17}$$

This equation has roots

$$\alpha_{1,2} = \frac{2\mathbf{d} \cdot (\mathbf{t}_1 + \mathbf{t}_2) \pm \sqrt{[2\mathbf{d} \cdot (\mathbf{t}_1 + \mathbf{t}_2)]^2 - 8(\mathbf{t}_1 \cdot \mathbf{t}_2 - 1)\mathbf{d} \cdot \mathbf{d}}}{4(\mathbf{t}_1 \cdot \mathbf{t}_2 - 1)}. \tag{3.18}$$

We modify the expression under the square root.

$$[2\mathbf{d} \cdot (\mathbf{t}_1 + \mathbf{t}_2)]^2 - 8(\mathbf{t}_1 \cdot \mathbf{t}_2 - 1)\mathbf{d} \cdot \mathbf{d} = \tag{3.19}$$
$$= 4\mathbf{d}^2\mathbf{t}_1^2 + 8\mathbf{d}^2\mathbf{t}_1 \cdot \mathbf{t}_2 + 4\mathbf{d}^2\mathbf{t}_2^2 - 8\mathbf{d}^2\mathbf{t}_1 \cdot \mathbf{t}_2 + 8\mathbf{d}^2 = \tag{3.20}$$
$$= 4\mathbf{d}^2\mathbf{t}_1^2 + 4\mathbf{d}^2\mathbf{t}_2^2 + 8\mathbf{d}^2, \tag{3.21}$$

which is always positive, therefore we always have real solutions. Moreover,

$$2\mathbf{d} \cdot (\mathbf{t}_1 + \mathbf{t}_2) \leq \sqrt{[2\mathbf{d} \cdot (\mathbf{t}_1 + \mathbf{t}_2)]^2 - 8(\mathbf{t}_1 \cdot \mathbf{t}_2 - 1)\mathbf{d} \cdot \mathbf{d}}, \tag{3.22}$$

because $\mathbf{t}_1 \cdot \mathbf{t}_2 \in \langle -1, 1 \rangle$. So if pick the root

$$\alpha = \frac{2\mathbf{d} \cdot (\mathbf{t}_1 + \mathbf{t}_2) - \sqrt{[2\mathbf{d} \cdot (\mathbf{t}_1 + \mathbf{t}_2)]^2 - 8(\mathbf{t}_1 \cdot \mathbf{t}_2 - 1)\mathbf{d} \cdot \mathbf{d}}}{4(\mathbf{t}_1 \cdot \mathbf{t}_2 - 1)}. \tag{3.23}$$

we get negative numerator and since the denominator is always negative, we get positive solution. This is important, since if we would have only negative α (and therefore negative β), we would get the points $\mathbf{A}_1, \mathbf{A}_2$ (see (3.1),(3.2)) in the opposite direction from $\mathbf{P}_1, \mathbf{P}_2$ then we want and we would get biarc interpolating data $(\mathbf{P}_1, -\mathbf{t}_1), (\mathbf{P}_2, -\mathbf{t}_2)$ instead of the data $(\mathbf{P}_1, \mathbf{t}_1), (\mathbf{P}_2, \mathbf{t}_2)$.

The choice of $\alpha = \beta$ has another advantage that special cases can easily be identified and computed from (3.17). There are three special cases :

1. $\mathbf{t}_1 \cdot \mathbf{t}_2 = 1$

   In this case, tangents $\mathbf{t}_1, \mathbf{t}_2$ are parallel. We can rewrite $(\mathbf{t}_1 + \mathbf{t}_2)$ as $2\mathbf{t}_1$ and (3.17) becomes

   $$\mathbf{d} \cdot \mathbf{d} - 4\alpha\mathbf{d} \cdot \mathbf{t}_1 = 0, \tag{3.24}$$

   with root

   $$\alpha = \frac{\mathbf{d} \cdot \mathbf{d}}{4\mathbf{d} \cdot \mathbf{t}_1}. \tag{3.25}$$

   Since $\mathbf{d} \cdot \mathbf{d}$ is always positive, we get a positive root, if $\mathbf{d} \cdot \mathbf{t}_1 > 0$, i.e., if the angle between chord $\mathbf{d}$ and tangent $\mathbf{t}_1$ is smaller than $\dfrac{\pi}{2}$. If $\mathbf{d} \cdot \mathbf{t}_1 < 0$, we have only negative α and we can use one of the variants below.

   Variant a)
   We use the negative α and set weight vector to

   $$W = \left\{ 1, -\cos\frac{\beta_1}{2}, 1, -\cos\frac{\beta_2}{2}, 1 \right\}. \tag{3.26}$$

   Then we get a biarc that consist of arcs that are greater then semicircle (see Figure 3.3).

   Variant b)
   We split the data to

   $$((\mathbf{P}_1, \mathbf{t}_1), (\mathbf{B}, \mathbf{t}_B)), \ ((\mathbf{B}, \mathbf{t}_B), (\mathbf{P}_2, \mathbf{t}_2)), \tag{3.27}$$
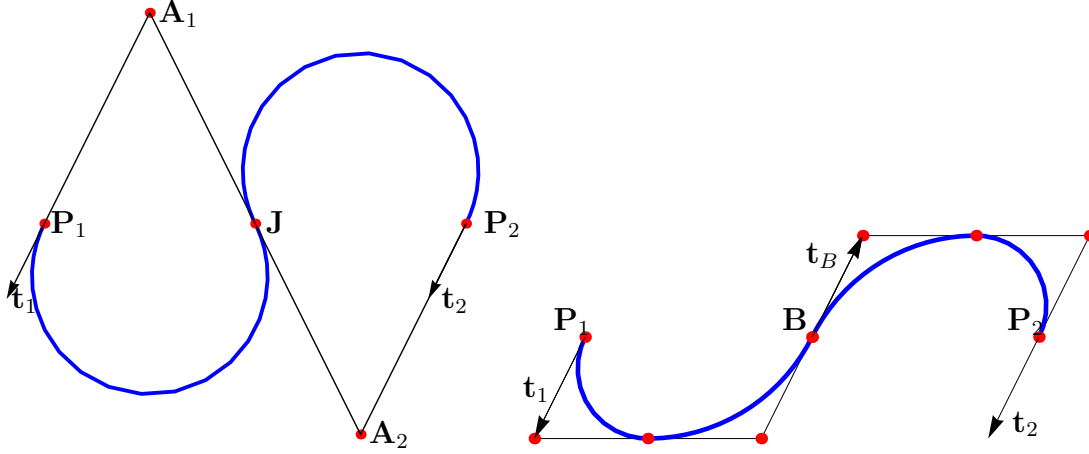
Figure 3.3: Special case 1: Parallel tangents such that $\mathbf{d} \cdot \mathbf{t}_1 < 0$ variant a) (left), variant b) (right) for the same point-tangent data pair.

where $\mathbf{B} = \dfrac{\mathbf{P}_1 + \mathbf{P}_2}{2}$ and $\mathbf{t}_B$ is antiparallel to $\mathbf{t}_1 = \mathbf{t}_2$. After interpolation of these two point-tangent data pairs, we get curve formed by two biarcs, i.e., four arcs (see Figure 3.3). Variant a) has disadvantage of negative weights and it gives biarc that is unnecesarily long, therefore it is usually more convenient to use variant b).

Moreover, if in this case $\mathbf{d} \cdot \mathbf{t}_1 = 0$, then we get 0 denominator in (3.25). This means that tangents $\mathbf{t}_1, \mathbf{t}_2$ are perpendicular to chord vector $\mathbf{d}$ and biarc consists of two semicircles (and therefore two points of control polygon "are at infinity"). This can be also solved by splitting the data as in variant b).

2. $\mathbf{t}_1 \cdot \mathbf{t}_2 = -1$

   In this case, tangents $\mathbf{t}_1, \mathbf{t}_2$ are antiparallel. Since also $\mathbf{t}_1 + \mathbf{t}_2 = 0$, (3.17) becomes

   $$\mathbf{d} \cdot \mathbf{d} - 4\alpha^2 = 0,$$

   which has roots

   $$\alpha = \pm \frac{\sqrt{\mathbf{d} \cdot \mathbf{d}}}{2} = \pm \frac{||\mathbf{d}||}{2}.$$

   So we can always pick the positive one.

3. $\mathbf{d} \cdot (\mathbf{t}_1 + \mathbf{t}_2) = 0$

   This means that the vector sum of tangents $\mathbf{t}_1, \mathbf{t}_2$ is perpendicular to the chord joining the end points. Again, we split the problem into interpolation of two point-tangent data pairs

   $$((\mathbf{P}_1, \mathbf{t}_1), (\mathbf{B}, \mathbf{t}_B)), \ ((\mathbf{B}, \mathbf{t}_B), (\mathbf{P}_2, \mathbf{t}_2)), \tag{3.28}$$

   where $\mathbf{B} = \dfrac{\mathbf{P}_1 + \mathbf{P}_2}{2}$ and $\mathbf{t}_B$ is perpendicular to $\mathbf{d}$ (c.f. Figure 3.5).
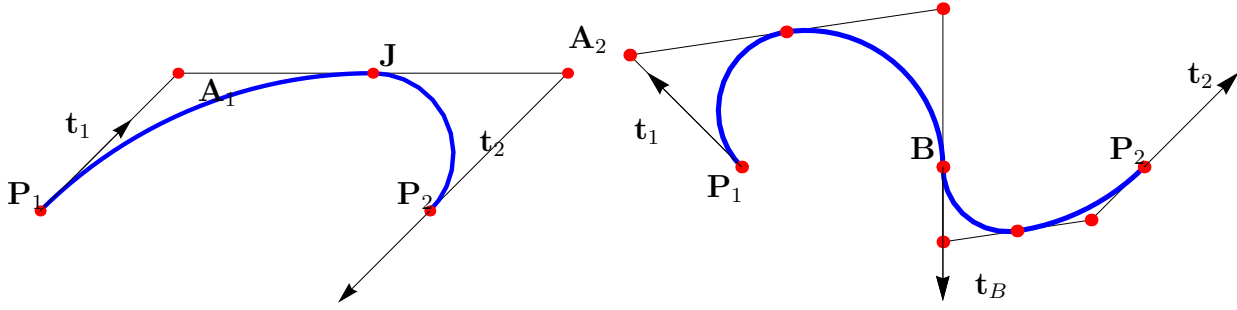
27

Figure 3.4: Special cases 2 and 3: Biarc with antiparallel tangents (left) and biarc with $\mathbf{d} \cdot (\mathbf{t}_1 + \mathbf{t}_2) = 0$ (right).

The procedure of constructing NURBS biarc with $\alpha = \beta$ is summarized in Algorithm 3.

Algorithm 3 nurbs$(\mathbf{P}_1, \mathbf{t}_1, \mathbf{P}_2, \mathbf{t}_2)$ returns control points, knot and weight vector

Inputs: $\mathbf{P}_1, \mathbf{t}_1, \mathbf{P}_2, \mathbf{t}_2$

1: Find positive α satisfying $\mathbf{d} \cdot \mathbf{d} - 2\alpha \mathbf{d} \cdot (\mathbf{t}_1 + \mathbf{t}_2) + 2\alpha^2 (\mathbf{t}_1 \cdot \mathbf{t}_2 - 1) = 0$

2: Determine remaining points of control polygon $\mathbf{A}_1 = \mathbf{P}_1 + \alpha \mathbf{t}_1$, $\mathbf{A}_2 = \mathbf{P}_2 - \alpha \mathbf{t}_2$,
$\mathbf{J} = \dfrac{1}{2} (\mathbf{A}_1 + \mathbf{A}_2)$

3: Determine knot vector $K = \{0, 0, 0, T, T, 1, 1, 1\}$, where $T = \dfrac{||\mathbf{J} - \mathbf{P}_1||}{||\mathbf{J} - \mathbf{P}_1|| + ||\mathbf{P}_2 - \mathbf{J}||}$

4: Determine weight vector $W = \left\{ 1, \dfrac{\cos \beta_1}{2}, 1, \dfrac{\cos \beta_2}{2}, 1 \right\}$, where $\beta_1 = \angle(\mathbf{P}_1 \mathbf{A}_1 \mathbf{J})$,
$\beta_2 = \angle(\mathbf{P}_2 \mathbf{A}_2 \mathbf{J})$

Returns: $\mathbf{A}_1, \mathbf{J}, \mathbf{A}_2, K, W$

3.3 Joining more NURBS biarcs together

We can also join two or more NURBS biarcs to one. Necessary condition that must be satisfied when joining two biarcs together is that the first biarc ends at the point where the second biarc starts and tangent at this point is the same. Therefore if the first biarc is interpolating point-tangent data pair $(\mathbf{P}_1, \mathbf{t}_1, \mathbf{P}_2, \mathbf{t}_2)$ then the second one must interpolate $(\mathbf{P}_2, \mathbf{t}_2, \mathbf{P}_3, \mathbf{t}_3)$.

Let us have two NURBS biarcs, the first one described by

$$\{\mathbf{P}_1, \mathbf{A}_1, \mathbf{J}_1, \mathbf{A}_2, \mathbf{P}_2\}, \tag{3.29}$$

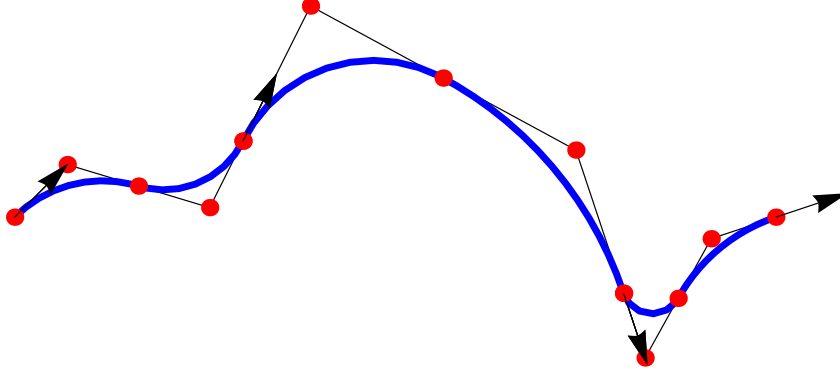$$W_1 = \left\{ 1, \frac{\cos \beta_1}{2}, 1, \frac{\cos \beta_2}{2}, 1 \right\}, \tag{3.30}$$

28

Figure 3.5: Three NURBS biarcs joined together

$$K_1 = \{0, 0, 0, T_1, T_1, 1, 1, 1\}, \tag{3.31}$$

$$T_1 = \frac{|\mathbf{P}_1\mathbf{J}_1|}{|\mathbf{P}_1\mathbf{J}_1| + |\mathbf{J}_1\mathbf{P}_2|}, \tag{3.32}$$

and the second one by

$$\{\mathbf{P}_2, \mathbf{A}_3, \mathbf{J}_2, \mathbf{A}_4, \mathbf{P}_3\}, \tag{3.33}$$

$$W_2 = \left\{1, \frac{\cos\beta_3}{2}, 1, \frac{\cos\beta_4}{2}, 1\right\}, \tag{3.34}$$

$$K_2 = \{0, 0, 0, T_2, T_2, 1, 1, 1\}, \tag{3.35}$$

$$T_2 = \frac{|\mathbf{P}_2\mathbf{J}_2|}{|\mathbf{P}_2\mathbf{J}_2| + |\mathbf{J}_2\mathbf{P}_3|}. \tag{3.36}$$

These two NURBS biarcs can be described as one by control polygon

$$\{\mathbf{P}_1, \mathbf{A}_1, \mathbf{J}_1, \mathbf{A}_2, \mathbf{P}_2, \mathbf{A}_3, \mathbf{J}_2, \mathbf{A}_4, \mathbf{P}_3\}, \tag{3.37}$$

weight vector

$$W = \left\{1, \frac{\cos\beta_1}{2}, 1, \frac{\cos\beta_2}{2}, 1, \frac{\cos\beta_3}{2}, 1, \frac{\cos\beta_4}{2}, 1\right\}, \tag{3.38}$$

and knot vector

$$K = \left\{0, 0, 0, \frac{T_1}{2}, \frac{T_1}{2}, \frac{1}{2}, \frac{1}{2}, \frac{1+T_2}{2}, \frac{1+T_2}{2}, 1, 1, 1\right\}. \tag{3.39}$$

We can join more then two NURBS biarc together. Again the condition of continuous data must be satisfied, i.e. following biarc must start where the previous biarc ended with the same tangent at this point. Let n be the number of biarcs we want to join, then i-th biarc is defined by control polygon

$$\{\mathbf{P}_i, \mathbf{A}_{2i-1}, \mathbf{J}_i, \mathbf{A}_{2i}, \mathbf{P}_{i+1}\}, \tag{3.40}$$

29

with weight vector

$$\{1, w_{2i-1}, 1, w_{2i}, 1\} \tag{3.41}$$

and knot vector

$$\{0, 0, 0, T_i, T_i, 1, 1, 1\}. \tag{3.42}$$

To describe n NURBS biarcs as one NURBS curve, we set control polygon to be

$$\left\{\{\mathbf{P}_i, \mathbf{A}_{2i-1}, \mathbf{J}_i, \mathbf{A}_{2i}\}_{i=1}^n, \mathbf{P}_{n+1}\right\}. \tag{3.43}$$

Weight vector of resulting NURBS curve can be written as

$$W = \left\{\{1, w_{2i-1}, 1, w_{2i}\}_{i=1}^n, 1\right\} \tag{3.44}$$

and knot vector as

$$K = \left\{0, 0, \left\{\frac{i-1}{n}, \frac{i-1+T_i}{n}, \frac{i-1+T_i}{n}, \frac{i}{n}\right\}_{i=1}^n, 1, 1\right\}. \tag{3.45}$$

3.4   NURBS biarc in space

NURBS description of biarc has great advatage of simple generalization to higher dimension. We can construct NURBS biarc in $\mathbb{R}^3$ by the exactly same procedure as in plane. The only change is that in this case we work with 3 coordinates, but the formulas for control points, weight vector and knot vector remain the same. Again, we can join more NURBS biarcs in one by (3.43), (3.44) and (3.45).
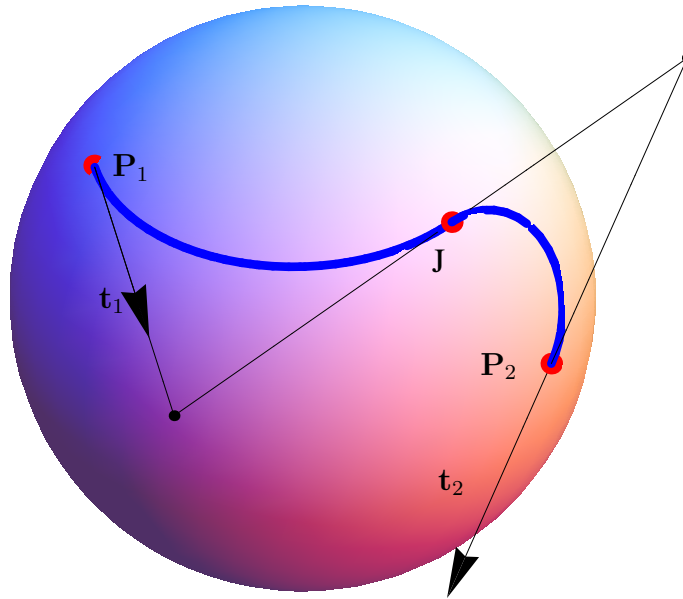

Figure 3.6: Spatial NURBS biarc

Chapter 4

Choosing a joining point

In this chapter we will discuss some possible choices of joining point of biarc and its effect on the resulting shape and curvature of the biarc.

4.1 Equal-chord biarc

The equal-chord biarc is often used in practice, since it forms nicely shaped biarc. It is constructed so that the two segments $\mathbf{P_1J}$ and $\mathbf{JP_2}$ have the same length. First, we construct locus circle l of all possible joining points as in Theorem 1.1.2. Since we want the distance $\mathbf{P_1J}$ to be the same as the distance $\mathbf{JP_2}$, we find $\mathbf{J}$ as intersection of bisector of $\mathbf{P_1P_2}$ and locus circle l (see Figure 4.1). Once we have a joining point, we construct biarc as described in Chapter 2.
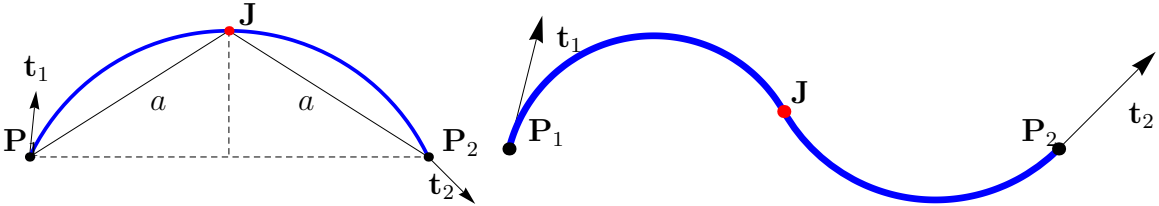

Figure 4.1: Finding a joining point of equal-chord biarc (left). Example of equal-chord biarc (right).

4.2 Parallel-tangent biarc as NURBS

We can use NURBS formulation to construct the so called parallel-tangent biarc. This biarc has such property that tangent $\mathbf{t_J}$ at joining point $\mathbf{J}$ is parallel to chord $\mathbf{P_1P_2}$. Parallel-tangent biarc can only be C-shaped (see Definition 1.1.2), therefore the point-tangent data pair must satisfy condition that the angles ϕ_1, ϕ_2 between tangent vectors and chord vector

have the opposite sign.

We require that NURBS has all properties as in Chapter 3 and we will add one more property. Let $\mathbf{t}_J$ be a unit vector from $\mathbf{A}_1$ to $\mathbf{J}$ (i.e., also from $\mathbf{J}$ to $\mathbf{A}_2$):

$$\mathbf{t}_J = \frac{\mathbf{J} - \mathbf{A}_1}{||\mathbf{J} - \mathbf{A}_1||} = \frac{\mathbf{J} - \mathbf{A}_1}{\alpha}. \tag{4.1}$$

For tangent $\mathbf{t_J}$ at joining point $\mathbf{J}$ to be parallel to chord $\mathbf{P}_1\mathbf{P}_2$, the following must hold

$$\mathbf{t}_J = \mathbf{e} = \frac{\mathbf{P}_2 - \mathbf{P}_1}{||\mathbf{P}_2 - \mathbf{P}_1||}, \tag{4.2}$$

where $\mathbf{e}$ is the unit chord vector. We plug (4.1) to (4.2) and get

$$\frac{\mathbf{J} - \mathbf{A}_1}{\alpha} - \mathbf{e} = 0.$$

Next, we replace $\mathbf{J} - \mathbf{A}_1$ by (3.10)

$$\frac{-\dfrac{\alpha}{\alpha + \beta} \cdot (-\mathbf{d} + \alpha\mathbf{t}_1 + \beta\mathbf{t}_2)}{\alpha} - \mathbf{e} = 0,$$

and modify

$$-\frac{1}{\alpha + \beta} \cdot (-\mathbf{d} + \alpha\mathbf{t}_1 + \beta\mathbf{t}_2) - \mathbf{e} = 0,$$
$$\mathbf{d} - \alpha\mathbf{t}_1 - \beta\mathbf{t}_2 - \alpha\mathbf{e} - \beta\mathbf{e} = 0,$$
$$\beta = \frac{(\mathbf{d} - \alpha(\mathbf{t}_1 + \mathbf{e})) \cdot (\mathbf{t}_2 + \mathbf{e})}{(\mathbf{t}_2 + \mathbf{e}) \cdot (\mathbf{t}_2 + \mathbf{e})}. \tag{4.3}$$

Equation (4.3) gives relation between α and β that must hold in order to construct a "parallel-tangent" biarc.

4.3   Minimizing the difference in curvatures

We can choose joining point $\mathbf{J}$ in such a way that we obtain a curve with the best local smoothness. This means that absolute difference

$$\triangle k = |k_2 - k_1|$$

of the curvatures k_1 and k_2 of the two arcs is minimal. In practice, minimizing the difference of curvatures of the two arcs minimizes vibrations of the rotating cam of NC machine.
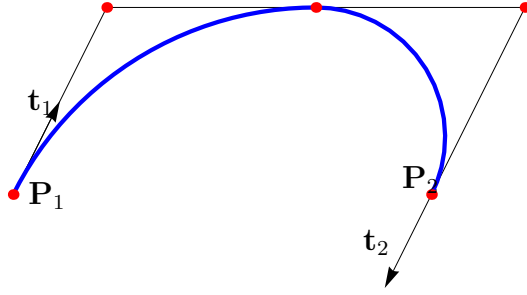
Figure 4.2: "Parallel-tangent" biarc

Let us again have the point-tangent data pair $(\mathbf{P}_1, \mathbf{t}_1), (\mathbf{P}_2, \mathbf{t}_2)$ that we wish to interpolate by a biarc curve. This means that the distance between the centres $\mathbf{M}_1$ and $\mathbf{M}_2$ of the circles must be equal to the absolute difference of the radii $|r_1 - r_2|$ of the two circular arcs. This can be expressed as (c.f. [11]):

$$\left(r_1 \cdot \mathbf{n}_1 - r_2 \cdot \mathbf{n}_2 - \delta \mathbf{e}\right)^2 = (r_1 - r_2)^2, \tag{4.4}$$

where $\mathbf{n}_1, \mathbf{n}_2$ are the unit normal vectors at the points $\mathbf{P}_1, \mathbf{P}_2$, $\mathbf{e}$ is the unit vector directed from $\mathbf{P}_1$ to $\mathbf{P}_2$ and δ is the distance between the points $\mathbf{P}_1$ and $\mathbf{P}_2$. After modification of (4.4), we can express radius r_2 in terms of r_1:

$$r_2 = \frac{r_1 \delta \mathbf{n}_1 \cdot \mathbf{e} - \dfrac{\delta^2}{2}}{\delta \mathbf{n}_2 \cdot \mathbf{e} + r_1(1 - \mathbf{n}_1 \cdot \mathbf{n}_2)}. \tag{4.5}$$

It is well known that curvature of a circle is constant and it is reciprocal of radius of the circle. Considering this, we can rewrite (4.5) as

$$k_2 = \frac{k_1 \delta \mathbf{n}_2 \cdot \mathbf{e} + 1 - \mathbf{n}_1 \cdot \mathbf{n}_2}{\delta \mathbf{n}_1 \cdot \mathbf{e} - k_1 \dfrac{\delta^2}{2}}. \tag{4.6}$$

We can replace scalar products of normal vectors $\mathbf{n}_1, \mathbf{n}_2$ and vector $\mathbf{e}$ by trigonometric functions using angles α_1, α_2 (see Figure 4.3) :

$$k_2 = \frac{-k_1 \delta \sin \alpha_2 + 1 - \cos(\alpha_1 - \alpha_2)}{\delta \sin \alpha_1 - k_1 \frac{\delta^2}{2}}. \tag{4.7}$$

Radii r_1, r_2 (resp. curvatures k_1, k_2) and angles α_1, α_2 can also have a negative sign. Radius r_1 is positive if $\mathbf{P}_1 \mathbf{M}_1$ has the same direction as $\mathbf{n}_1$ (analogously for r_2). Sign of α_1, α_2 depends on its orientation from $\mathbf{P}_1, \mathbf{P}_2$. In Figure 4.3, α_1 is negative, α_2 is positive, and r_1 and r_2 are positive.

Now we want to minimize the difference between curvatures

$$\triangle k = |k_1 - k_2|,$$

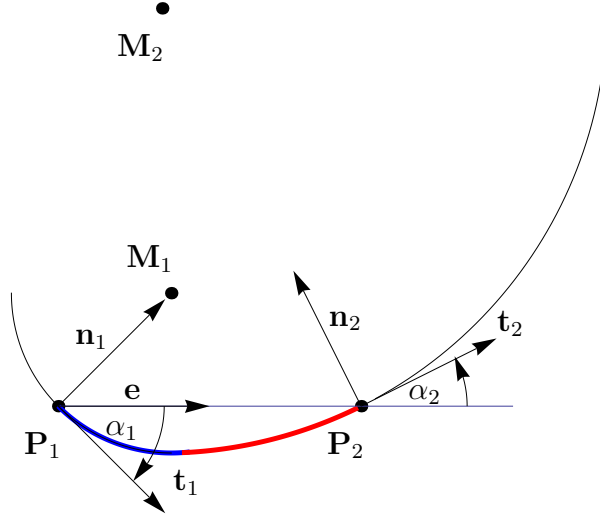Figure 4.3: Angles α_1, α_2

which is equivalent to solving the equation

$$\frac{dk_1}{dk_2} = 1. \tag{4.8}$$

Putting together (4.6) and (4.8) we get (c.f. [11])

$$k_1^* = \frac{2}{\delta} \left[\mathbf{n}_1 \cdot \mathbf{e} \pm \sqrt{(\mathbf{n}_1 \cdot \mathbf{e})(\mathbf{n}_2 \cdot \mathbf{e}) + \frac{1 - \mathbf{n}_1 \cdot \mathbf{n}_2}{2}} \right], \tag{4.9}$$

$$k_2^* = -\frac{2}{\delta} \left[\mathbf{n}_2 \cdot \mathbf{e} \pm \sqrt{(\mathbf{n}_2 \cdot \mathbf{e})(\mathbf{n}_2 \cdot \mathbf{e}) + \frac{1 - \mathbf{n}_1 \cdot \mathbf{n}_2}{2}} \right]. \tag{4.10}$$

which are expressions for optimal curvatures that minimize $\triangle k = |k_1 - k_2|$. The variable sign $\pm$ is chosen so that k_1^*, k_2^* are minimum of $\triangle k = |k_1 - k_2|$, not maximum. We can again replace scalar products with trigonometric functions and get expressions for minimizing difference in curvatures of the two arcs

$$k_1^* = -\frac{2}{\delta} \left(\sin \alpha_1 + \sin \frac{\alpha_1 + \alpha_2}{2} \right), \tag{4.11}$$

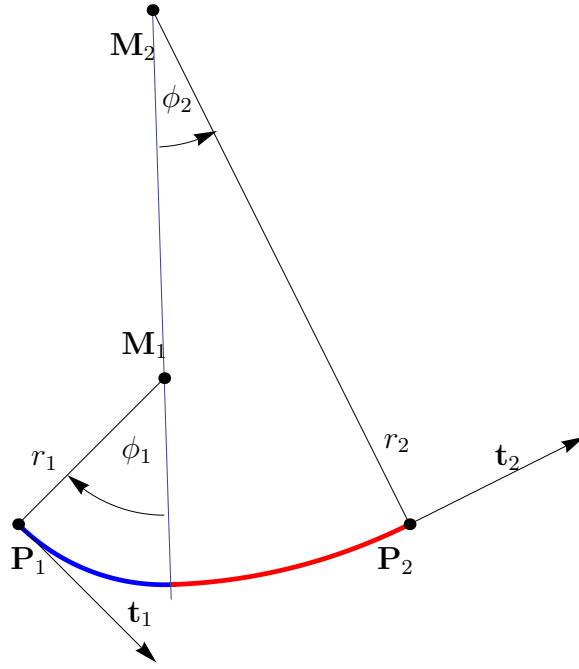$$k_2^* = \frac{2}{\delta} \left(\sin \alpha_2 + \sin \frac{\alpha_1 + \alpha_2}{2} \right). \tag{4.12}$$

34

Figure 4.4: Angles ϕ_1, ϕ_2

Optimal k_1^*, k_2^* also provides low value of the strain energy which can be expressed as integral

$$E = \int_l k^2 ds, \tag{4.13}$$

where l is the length of a curve. For biarc curve, (4.13) can be expressed as

$$E = \frac{\phi_1}{r_1} + \frac{\phi_2}{r_2}, \tag{4.14}$$

where angles ϕ_1, ϕ_2 correspond to length of arcs a_1, a_2 (see Figure 4.4).

Figure 4.5 shows four different biarcs for one point-tangent data pair and Table 4.1 shows values of energy strain integrals of these biarcs. Biarc $\mathbf{b}_1$ was constructed by the above description to minimize the difference in curvatures.
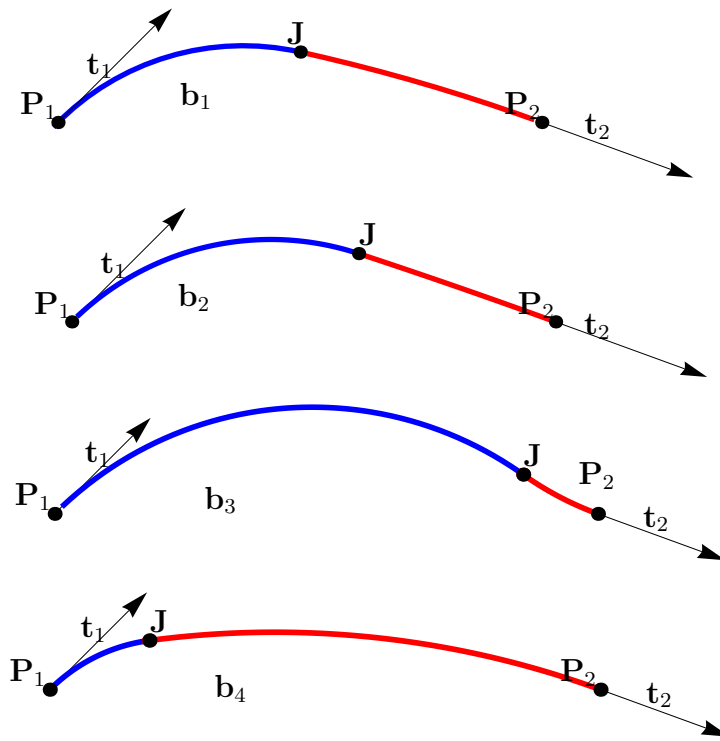
Figure 4.5: Various biarcs for the same point-tangent data pair and values of energy strain integral E, the first one minimizes E.

biarc	energy strain integral value
b_1	1.19187
b_2	1.84039
b_3	2.45102
b_4	2.26468

Table 4.1: Table of energy strain integral values.

4.4   Joining point on the curve

When we approximate given curve by biarcs (more about approximation of curve in Chapter 5), we can choose the joining point **J** to lie on the curve (c.f. [16]), i.e., we set **J** to be the intersection of given curve with locus of all possible joining points (see Figure 4.6). "**J** on the curve" method cannot be used for interpolation of data, it can only be used when we are approximating a curve (since we need a curve to be given). This choice typically produces a biarc which is closer to the original curve $\mathbf{c}(s)$ than those produced by other methods, because in this case not only $\mathbf{P}_1$ and $\mathbf{P}_2$ lie on the curve, but also **J**. Biarc then better follows the shape of the curve and the error is reduced. Example of approximation by biarcs with this choice of joining point will also be given in Chapter 5.
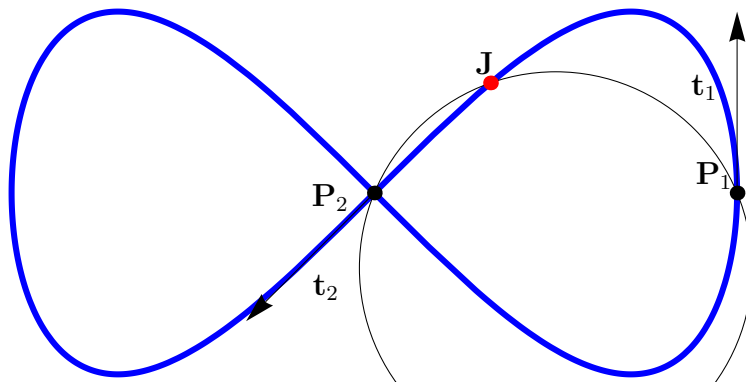

Figure 4.6: Joining point **J** as an intersection of locus circle and given curve

Chapter 5

Approximation of a given curve

5.1 Construction of an approximating biarc

In this chapter, we will discuss approximation of a given curve by piecewise circular spline curve composed of biarcs when accuracy is given. Let us have given accuracy ϵ, parametric equation of a curve $\mathbf{c}(s)$ where $s \in \langle 0, 1 \rangle$. We get coordinates of points $\mathbf{P}_1$ and $\mathbf{P}_2$ as

$$\mathbf{P}_1 = \mathbf{c}(0), \quad \mathbf{P}_2 = \mathbf{c}(1). \tag{5.1}$$

We can also estimate tangents at these two points as

$$\mathbf{t}_1 = \frac{\mathbf{c}'(0)}{||\mathbf{c}'(0)||}, \quad \mathbf{t}_2 = \frac{\mathbf{c}'(1)}{||\mathbf{c}'(1)||}. \tag{5.2}$$

We find a biarc through point-tangent data pair $(\mathbf{P}_1, \mathbf{t}_1), (\mathbf{P}_2, \mathbf{t}_2)$. Next, we compute the error of approximation (how to compute the error will be shown in next section). If the error is smaller than given accuracy, we are done. Otherwise we double (or increase in another way) the amount of points used, i.e., we split the data to

$$\left(\mathbf{c}(s), 0, \frac{1}{2} \right) \tag{5.3}$$

and

$$\left(\mathbf{c}(s), \frac{1}{2}, 1 \right) \tag{5.4}$$

and repeat. The above procedure can be summarized as Algorithm 4: $approxCurve(\mathbf{c}(s), \epsilon)$ (c.f. [16]).

In practice, we can also modify the approximation method in a way that once a segment of a curve has error smaller than the given tolerance, we leave it like that and we subdivide only those parts of the curve with errors larger than the given tolerance.

Algorithm 4 $approxCurve(\mathbf{c}(s), \epsilon)$

---

   n=1
   while error $> \epsilon$ **do**
      construct biarcs through $\left(\mathbf{c}(s), \dfrac{i-1}{n}, \dfrac{i}{n}\right)$ for $i = 1...n$
      $n = 2n$
   end while
   Return constructed biarcs

5.2 Error measure

To measure the error we can use

$$\delta_1 = \max_{t \in \langle 0,1 \rangle} ||\mathbf{c}(t) - \mathbf{b}(t)||, \tag{5.5}$$

where $\mathbf{b}(t)$ is a parametrization of biarc, $t \in \langle 0, 1 \rangle$. This error measure has the advantage of fast computations but it is not always accurate. Better way to measure the distance between two curves is by the Hausdorff distance

$$\delta_2 = \max_{s \in \langle 0,1 \rangle} \left\{ \min_{t \in \langle 0,1 \rangle} ||\mathbf{c}(s) - \mathbf{b}(t)||, \min_{t \in \langle 0,1 \rangle} ||\mathbf{b}(t) - \mathbf{c}(s)|| \right\} \tag{5.6}$$

Hausdorff distance usually gives more accurate result if we use sufficiently many points, but can be very slow. For example for just 100 sampled points on the curve, 20 000 distances need to be computed.

There is another good technique how to measure distance of a biarc from curve – one-sided Hausdorff distance with exploited fact, that we approximate the curve with circles, whose centres can be easily computed (c.f. [16]). Centre of a circle through $\mathbf{A}$ and $\mathbf{B}$ with unit tangent vector $\mathbf{t}$ at $\mathbf{A}$ is given by (see Theorem 2.1.1)

$$\mathbf{C} = \frac{\mathbf{A} + \mathbf{B}}{2} + \frac{||\mathbf{B} - \mathbf{A}||}{2 \tan \alpha} \mathbf{n}, \tag{5.7}$$

where α is the angle between tangent vector $\mathbf{t}$ and chord vector $\mathbf{e} = \dfrac{\mathbf{B} - \mathbf{A}}{||\mathbf{B} - \mathbf{A}||}$ and $\mathbf{n}$ is vector perpendicular to $\mathbf{e}$. One-sided Hausdorff distance between the curve and the biarc is then given as

$$\delta_3 = \max_{i,j} |r_i - ||\mathbf{C}_i - \mathbf{c}(s_j)|||, \ i = 1, ...n, \ j = \frac{1}{N}, ..., \frac{N-1}{N} \tag{5.8}$$

where $r_i, \mathbf{C}_i$ are radius and centre of $i-th$ arc and n is number of interpolating arcs, N is number of distances computed. For higher N we get more accurate result. Usually it is sufficient to take $N = 200$. We can use this error measure also in $\mathbb{R}^3$, where centre of interpolating arc through points $\mathbf{A}, \mathbf{B}$ with unit tangent vector $\mathbf{t}$ at $\mathbf{A}$ is given as intersection of three planes – see Theorem 2.1.2.
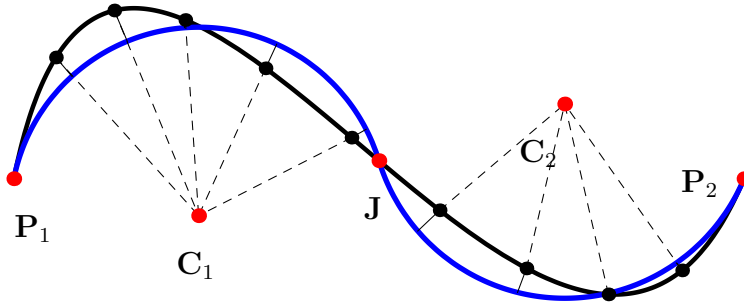
Figure 5.1: One-sided Hausdorff distance

5.3 Example of approximation

In this section we show how we approximated given curve by biarcs with two different choices of joining point. First by "$\alpha = \beta$ NURBS biarcs" (see Section 3.2) and then by "$\mathbf{J}$ on the curve biarcs" (see Section 4.4). We have approximated curve with parametrization

$$\mathbf{c}(s) = (2\cos{(2\pi s)},\ \sin{(4\pi s)}), \quad s \in (0,1). \tag{5.9}$$

It is a symmetric curve, therefore it is convenient to choose odd number of approximating biarcs in order to get again symmetric curve. Comparisson of approximation by the two methods can be seen in Figure 5.2 and in Table 5.1. We can see that the approximation with the choice of $\mathbf{J}$ on the curve is closer to the original curve.

number of biarcs	Hausdroff distance error	
	NURBS	$\mathbf{J}$ on the curve
2	0.30636	0.30636
4	0.36031	0.23076
8	0.05713	0.01872
12	0.01084	0.00761

Table 5.1: Error values of approximation of curve $\mathbf{c}(s) = (2\cos{(2\pi s)},\ \sin{(4\pi s)})$.
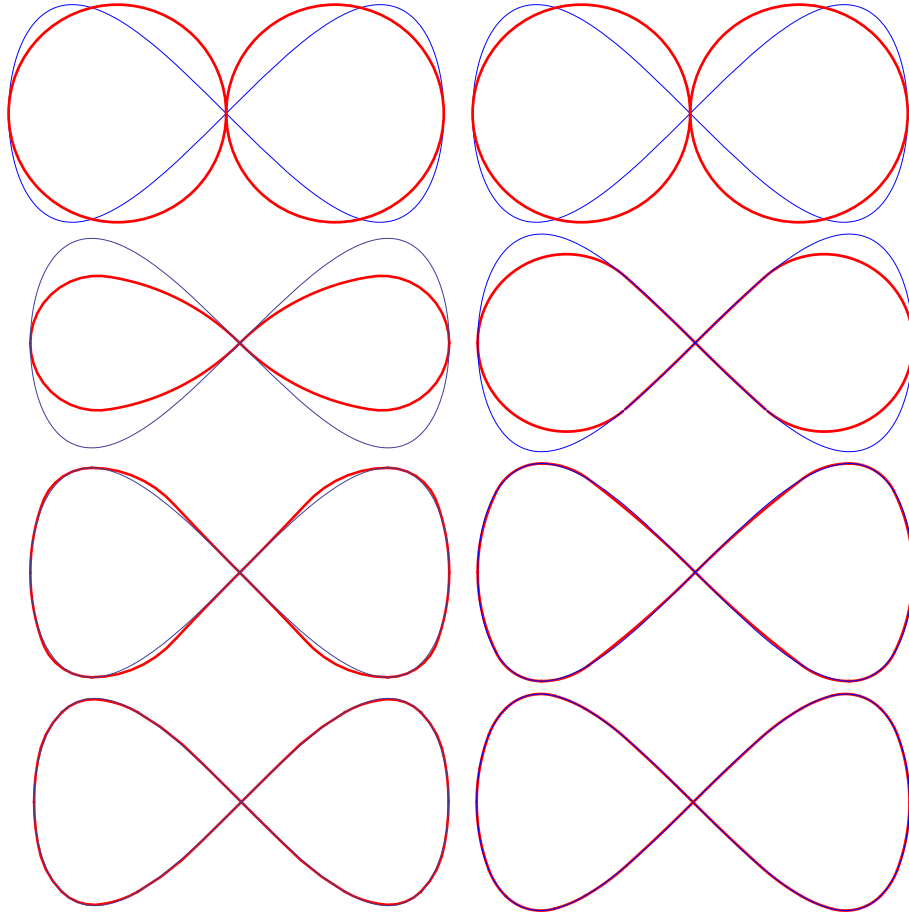
Figure 5.2: Approximation of curve $\mathbf{c}(s) = (2\cos(2\pi s),\ \sin(4\pi s))$ by 2,4,8 and 12 biarcs, respectively. Curve is shown in blue, approximation in red. Images on the left show approximation by NURBS biarc with $\alpha = \beta$, images on the right show approximation by biarcs with joining point $\mathbf{J}$ on the curve.

5.4 Order of approximation of equal chord method

In this section we derive the order of approximation by equal-chord biarcs. We have approximated cubic Bézier curve in $\mathbb{R}^2$ with control points $(0,0), (30, 150), (250, 120), (300, 0)$ (see Figure 5.3). Table 5.2 shows error depending on the number of biarcs used. It also shows the ratio of two consecutive errors. To measure the distance between approximating piecewise circular spline and the original curve we have used one-sided Hausdorff distance (5.8) estimated as maximum of 200 distances. We can see that gradually, when we double the number of biarcs the improvement ratio tends to 2^3, therefore the approximation order of method is three. We have also approximated cubic Bézier curve in $\mathbb{R}^3$ space with control points $(0,0,0), (-20, 150, -120), (300, -100, 80), (350, 100, 240)$ (see Figure 5.3). Also in $\mathbb{R}^3$ space the improvement ratio tends to 2^3 and the order of approximation is 3.
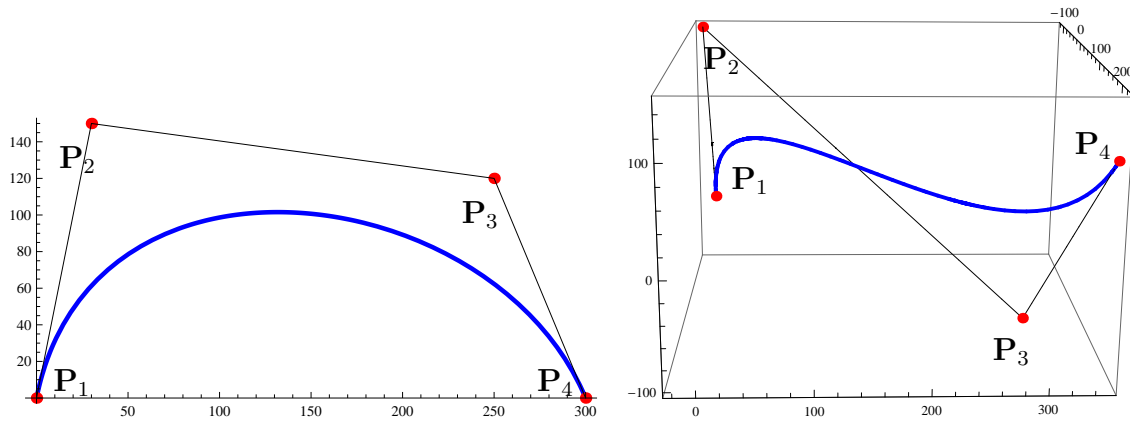
Figure 5.3: Cubic Bézier curve in $\mathbb{R}^2$ with control points $(0, 0),(30, 150),(250, 120),(300, 0)$ (left). Cubic Bézier curve in $\mathbb{R}^3$ with control points $(0, 0, 0)$, $(-20, 150, -120)$, $(300, -100, 80)$, $(350, 100, 240)$ (right).

$\mathbb{R}^2$ case			$\mathbb{R}^3$ case		
n	error	ratio	n	error	ratio
2	2.34193	—	2	11.5458	—
4	$2.96854 \cdot 10^{-1}$	7.88929	4	2.81163	4.10643
8	$2.74816 \cdot 10^{-2}$	10.8018	8	$7.80422 \cdot 10^{-1}$	3.60271
16	$3.35979 \cdot 10^{-3}$	8.17956	16	$4.94903 \cdot 10^{-2}$	15.7692
32	$4.43687 \cdot 10^{-4}$	7.57244	32	$4.81318 \cdot 10^{-3}$	10.2822
64	$5.78451 \cdot 10^{-5}$	7.66948	64	$5.23239 \cdot 10^{-4}$	9.19882
128	$7.33738 \cdot 10^{-6}$	7.88442	128	$5.97143 \cdot 10^{-5}$	8.76238
256	$9.22435 \cdot 10^{-7}$	7.95436	256	$7.12711 \cdot 10^{-6}$	8.37848
512	$1.15589 \cdot 10^{-7}$	7.98028	512	$8.70485 \cdot 10^{-7}$	8.18751
1024	$1.44655 \cdot 10^{-8}$	7.99071	1024	$1.0756 \cdot 10^{-7}$	8.09305

Table 5.2: Table of one-sided Hausdorff distances between original curve and approximating piecewise circular spline consisted of n biarcs in $\mathbb{R}^2$ and $\mathbb{R}^3$ and improvement ratio.

Chapter 6

Application of piecewise circular curves

6.1 Approximation of intersection of two natural surfaces

Mechanical parts may be classified in two broad groups:

- sculptured or free-form objects, e.g., car bodies, characterized by doubly curved bounding surfaces,

- unsculptured or functional objects, e.g., machine-tool components.

Part surveys show that a large proportion of parts are unsculptured, and that many of these are bounded by planes, cylinders, spheres, cones, tori, and blends between such surfaces (c.f. [10]). Planar, cylindrical, spherical, and conical surfaces are often called the natural quadrics, because they are produced easily by the usual machining operations. The curves that result from intersections of these surfaces generally cannot be expressed in closed form, therefore these curves of intersection are usually approximated by cubic splines that interpolate points lying on the true intersections. Cubic splines provide second-degree continuity, but they are expensive in computations. In this section we will show how to approximate intersection curves of natural surfaces by piecewise circular spline curves, trading second-degree continuity for computational simplicity (method taken from [10]).

Natural surface $\mathbf{F}(u, v)$ can be parametrized in such way, that if we successively keep fixing one parameter, we get parametric description of lines or circles called generators (see Figure 6.1) defined by

$$\mathbf{F}(u_0, v), \mathbf{F}(u, v_0), \tag{6.1}$$

where u_0, v_0 are constants. For example let us have cone with parametric description

$$\mathbf{F}(u, v) = \left\{ \frac{h - u}{h} r \cos v, \frac{h - u}{h} r \sin v, u \right\}, \tag{6.2}$$
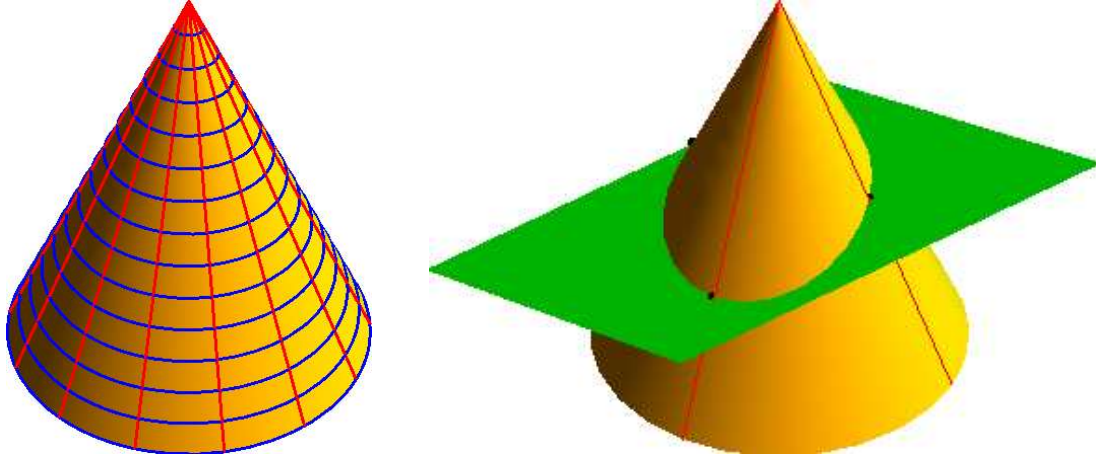
43

Figure 6.1: Line and circle generators we get if we fix one parameter in cone (left). Intersection of 4 cone line generators with plane (right).

where h is height and r is radius of the base. For fixed $v = v_0$ we get lines, for fixed $u = u_0$ circles. We use these generators when approximating intersection of two natural surfaces.

Let us have two natural surfaces $\mathbf{F}(u, v), \mathbf{G}(r, s)$ with parametric descriptions

$$\mathbf{F}(u, v),\ u \in (u_1, u_2), v \in (v_1, v_2),\ \mathbf{G}(r, s),\ r \in (r_1, r_2), s \in (s_1, s_2). \tag{6.3}$$

On surface $\mathbf{F}(u, v)$, we pick one set of generators (either $\mathbf{F}(u_0, v)$ or $\mathbf{F}(u, v_0)$) and we find intersection of this set with surface $\mathbf{G}(s, r)$. The more generators we use, the more intersecetion points we get, thus we get also better approximation.

After we have got intersection points, we also need tangents at these points. Tangent $\mathbf{t}_i$ at the point of intersection $\mathbf{P}_i$ can easily be calculated as

$$\mathbf{t}_i = \mathbf{n}_1^i \times \mathbf{n}_2^i, \tag{6.4}$$

where $\times$ denotes cross product and $\mathbf{n}_1^i, \mathbf{n}_2^i$ are normals at point $\mathbf{P}_i$ to surfaces $\mathbf{F}(u, v), \mathbf{G}(r, s)$, respectively. Once we have got sampled points and tangent vectors at these points, we can interpolate them by biarcs to get approximation of curve of intersection by piecewise circular curve. The above procedure can be written as Algorithm 6.1, where $\mathbf{F}(u, v_0)$ are used as generators. Algorithm for case when $\mathbf{F}_{(}u_0, v)$ are used would be analogical.
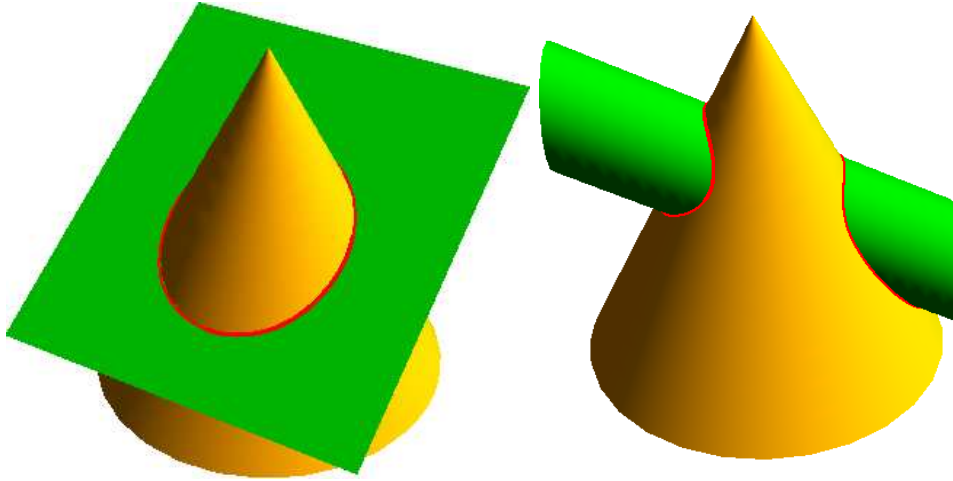
Figure 6.2: Approximation of intersection curve of cone with plane (4 generators used) and with cylinder (8 generators used).

Algorithm 5 *approxIntersect1* $(n, \mathbf{F}(u,v), \mathbf{G}(r,s))$ - approximate intersection of two natural surfaces

---

$n = N$ (set number of generators)

$\mathrm{V} = \left\{ v_1 + \dfrac{i-1}{n}(v_2 - v_1) \right\}_{i=1}^{n+1}$ (create sequence of parameter values $v = v_0$)

for $i = 1 \rightarrow n+1$ **do**
   $\mathbf{F}_i(u) = \mathbf{F}(u, V_i)$ (get generators)
end for
for $i = 1 \rightarrow n+1$ **do**
   Find $\mathbf{P}_i$ = intersection of $\mathbf{F}_i(u)$ with surface $\mathbf{G}(r,s)$
   Find tangent $\mathbf{t}_i = \mathbf{n}_1^i \times \mathbf{n}_2^i$
end for
for $i = 1 \rightarrow n$ **do**
   Construct biarc throught data $(\mathbf{P}_i, \mathbf{t}_i, \mathbf{P}_{i+1}, \mathbf{t}_{i+1})$
end for
if Intersection is closed curve **then**
   Construct biarc through data $(\mathbf{P}_{n+1}, \mathbf{t}_{n+1}, \mathbf{P}_1, \mathbf{t}_1)$
end if

6.2 Approximation of intersection of two rational surfaces

In this section we will show how to approximate the intersection curve of two rational parametric surfaces

$$\mathbf{S}_1(r, s), \ r \in (r_1, r_2), s \in (s_1, s_2), \tag{6.5}$$

$$\mathbf{S}_2(u, v), \ u \in (u_1, u_2), v \in (v_1, v_2) \tag{6.6}$$

by biarcs. We start by defining the rational parametric surface.

Definition 6.2.1. *We say that a surface $\boldsymbol{S}(r, s)$ is a rational parametric surface, if it can be written as*

$$\boldsymbol{S} = \left(\frac{p_1(r, s)}{q_1(r, s)}, \frac{p_2(r, s)}{q_2(r, s)}, \frac{p_3(r, s)}{q_3(r, s)} \right), \tag{6.7}$$

where p_i, q_i are polynomials in s and r and greatest common divisor of (p_i, q_i) satisfies

$$gcd(p_i, q_i) = 1, i = 1, 2, 3. \tag{6.8}$$

Next, we need an implicit equation of one of the surfaces. A common approach for implicitization is to consider the variety V in affine space $\mathbb{C}^{2+3}$ which is defined by equations (see [1])

$$q_1(r, s)x - p_1(r, s) = 0, \tag{6.9}$$

$$q_2(r, s)y - p_2(r, s) = 0, \tag{6.10}$$

$$q_3(r, s)z - p_3(r, s) = 0. \tag{6.11}$$

The variety V is interpreted as the graph of the parametrization (6.7). An implicit equation describes the algebraic relation over the coordinates x, y, z of the surface $\mathbf{S}$. So the implicitization process consists of finding algebraic combinations of the parametric equations (6.9),(6.10),(6.11), which eliminate the variables r and s. Notice, that $q_i(r, s) = 0$, $i = 1, 2, 3$ is allowed in (6.9),(6.10),(6.11), but not in (6.7). To ensure that $q_i(r, s) \neq 0$, we add another equation (called control polynomial)

$$1 - q_1(r, s)q_2(r, s)q_3(r, s)w = 0. \tag{6.12}$$

Now we apply Gröebner basis technique[1] to eliminate variables r, s, w from equations (6.9),(6.10),(6.11) and (6.12). More detailed description can be found in [1]. We have used *Wolfram Mathematica* function *GroebnerBasis*.

Let

$$F(x, y, z) = 0 \tag{6.13}$$

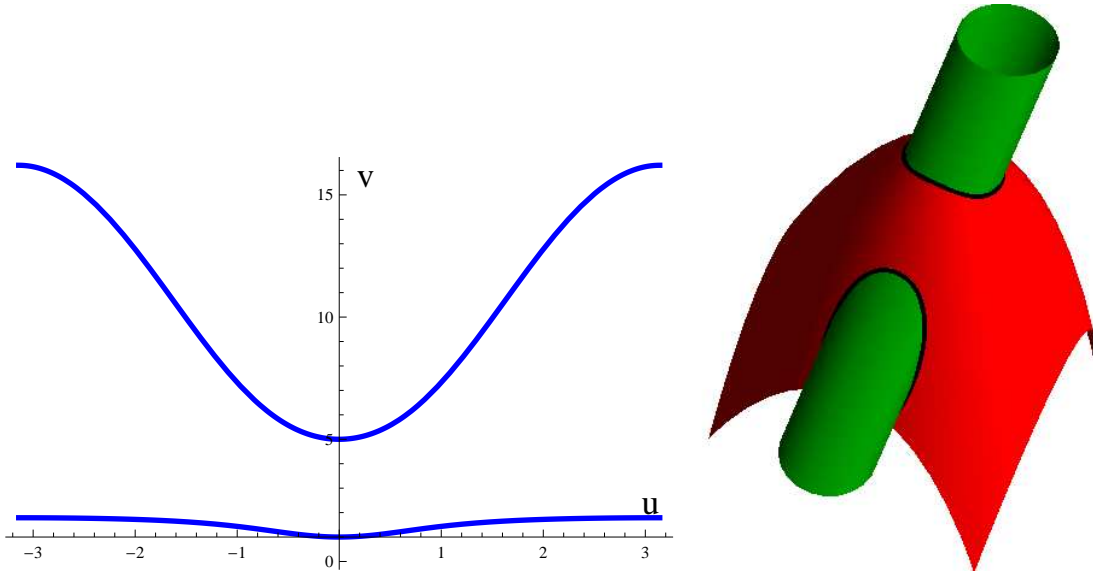[1]One can also apply methods that use resultants or characteristic set.

Figure 6.3: Implicit curve of intersection in (u, v) plane (left) and the corresponding actual curve of intersection in $\mathbb{R}^3$ (right)

be implicit equation of surface $\mathbf{S}_1$ we have got by the above mentioned method. We can now substitute the parametric equation of the surface $\mathbf{S}_2(u, v)$ into (6.13) to get implicitly given algebraic curve of intersection

$$f(u, v) = 0. \tag{6.14}$$

The topology of the curve (6.14) in the parameter plane (u, v) is important for us. The actual curve of intersection in $\mathbb{R}^3$ space has as many parts, as there are continuous parts of curve (6.14) in parameter plane (u, v). For example see Figure 6.3 - the intersection curve in (u, v) plane consists of two detached curves and therefore the intersection in $\mathbb{R}^3$ consists also of two detached curves. To determine the topology of the curve (6.14), we need to define division points.

Definition 6.2.2. *We say that a point $\boldsymbol{P}_0 = (u_0, v_0)$ is a division point if at least one partial derivative at this point is zero, i.e. if*

$$f_u(u_0, v_0) = 0 \tag{6.15}$$

or

$$f_v(u_0, v_0) = 0. \tag{6.16}$$

We divide the parameter domain $(u_1, u_2), (v_1, v_2)$ by horizontal and vertical lines going through every division point (see Figure 6.4). Horizontal and vertical lines through a point $\mathbf{P}_i$ are defined by

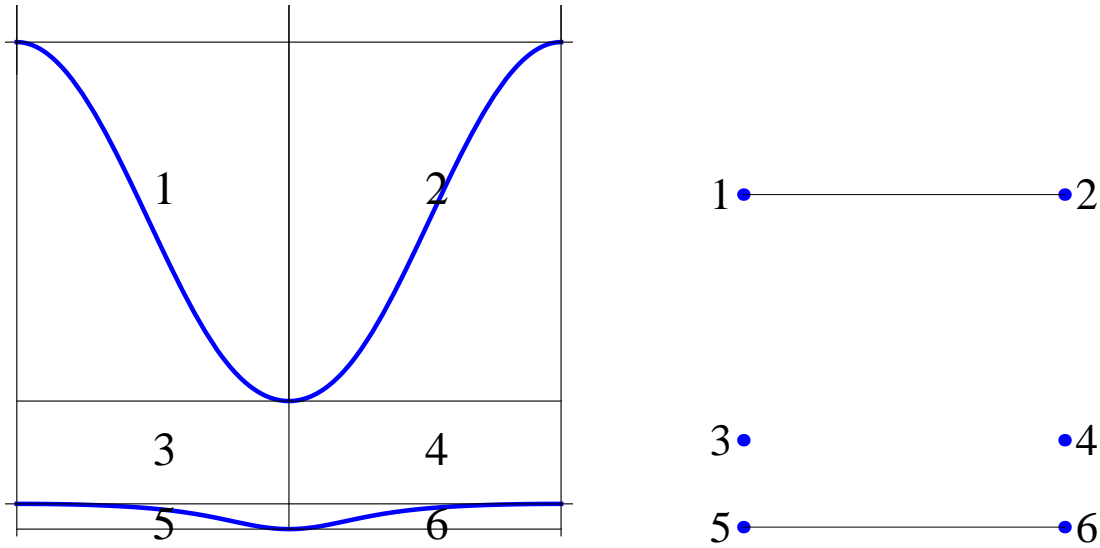$$p_H = \mathbf{P}_i + (1, 0)t, \ t \in \mathbb{R}, \tag{6.17}$$

47

Figure 6.4: Parameter domain division of the curve (left) and its topology graph (right).

$$p_V = \mathbf{P}_i + (0,1)t,\ t \in \mathbb{R}, \tag{6.18}$$

respectively. If the horizontal or vertical lines intersect the implicit curve (6.14), we add also these points of intersection to division points and construct another horizontal and veritcal lines through these points. This ensures that each of the boxes formed by these lines will contain maximally one continuous part of the curve (6.14). In general case, the number of horizontal and vertical lines will be the same and the domain is divided into $(n+1)^2$ boxes, where n is a number of division points. For every two division points that have the same u (resp. v) value and for every point that lies on the domain border, the number of vertical (resp. horizontal) lines decreases by one and we get $(h+1)(v+1)$ boxes, where h is number of horizontal lines and v is number of vertical lines.

We determine topology graph of the curve with respect to the division boxes. The topology graph consists of points and abscissae, where one point corresponds to curve segment in one box and line corresponds to continuity of curve between two boxes (see Figure 6.4).

Now we can start sampling points on the implicit curve of intersection $f(u,v) = 0$ in parameter plane (u,v). We take some starting point $\mathbf{P}_0 = (u_0, v_0)$. We choose this point to be the boundary point of one of the continuous parts of curve. We find a unit tangent vector at this point as

$$\mathbf{t}_0 = \frac{(f_u(u_0, v_0), -f_v(u_0, v_0))}{||(f_u(u_0, v_0), -f_v(u_0, v_0))||} \tag{6.19}$$
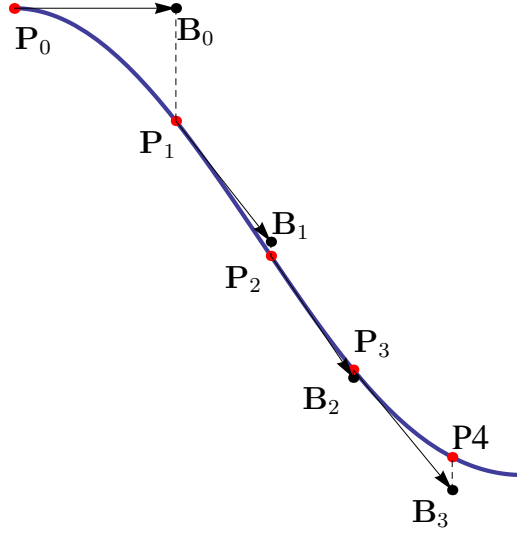
Figure 6.5: Newton's method for sampling points on the curve.

or if we need tangent vectors in opposite direction

$$\mathbf{t}_0 = \frac{(-f_u(u_0, v_0), f_v(u_0, v_0))}{||(-f_u(u_0, v_0), f_v(u_0, v_0))||}. \tag{6.20}$$

Now we set a point

$$\mathbf{B}_0 = \mathbf{P}_0 + \alpha \mathbf{t}_0, \ \alpha \in \mathbb{R}, \tag{6.21}$$

which is a point that is from point $\mathbf{P}_0$ at distance α in direction of $\mathbf{t}_0$. Therefore the point $\mathbf{B}_0$ does not (generally) lie on the curve $f(u,v) = 0$ but is "efficiently close" to it. We find a new point $\mathbf{P}_1$ on the curve by using for example Newton's method (see Figure 6.5). We choose α with respect to the parameter domain range and also with respect to how many points we want to sample on the curve. We set α smaller if we have small domain range or if we want more sampling points and we set α larger if we have large domain range or if we want less sampling points. To get similarly spaced sampling points we can set α to vary with respect to the tangent at a point - to increase when the slope is big and decrease when the slope is small. This applies especially for a curve that changes its slope rapidly.

We repeat this procedure until we have sampled the points on the whole one connected part of the curve and for all parts of the curve $f(u,v) = 0$. To find spatial coordinates we plug values (u,v) of sampled points to the equation of surface $\mathbf{S}_2(u,v)$. Tangent vectors at these points can be obtained again as cross product of gradient vectors

$$\mathbf{t}(u, v) = \nabla F(x, y, z) \times \mathbf{n}_2(u, v), \tag{6.22}$$

where $\nabla F = \left(\frac{\partial F}{\partial x}, \frac{\partial F}{\partial y}, \frac{\partial F}{\partial z} \right)$ and $\mathbf{n}_2 = \frac{\partial \mathbf{S}_2}{\partial u} \times \frac{\partial \mathbf{S}_2}{\partial v}$. Again, once we have got sampled points and tangent vectors at these points, we can interpolate them by biarcs to get ap-

proximation of curve of intersection by piecewise circular curve.
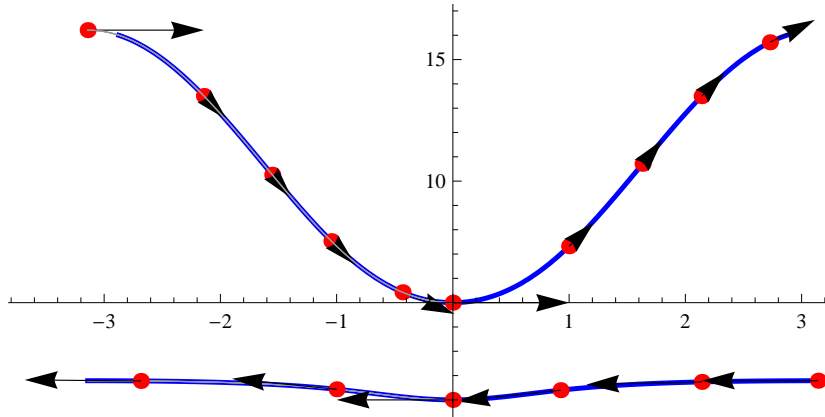

Figure 6.6: Sampled points in plane (u, v)

We have applied the above procedure to approximate the intersection of elliptic cylinder

$$\mathbf{S}_1 = (r, 3 \sin s, -2 + r + 3 \cos s) \tag{6.23}$$

and elliptic paraboloid

$$\mathbf{S}_2 = \left(\frac{u^2 + v^2 + 1}{2}, 2u, 2v \right). \tag{6.24}$$

Figure 6.6 shows sampled points in parameter plane (u, v) of implicit curve of intersection

$$-4 + 8u - (-2 + u + 3 \cos v)^2 - 9(\sin v)^2 = 0 \tag{6.25}$$

and Figure 6.7 shows approximation of intersection of these two surfaces by this method.
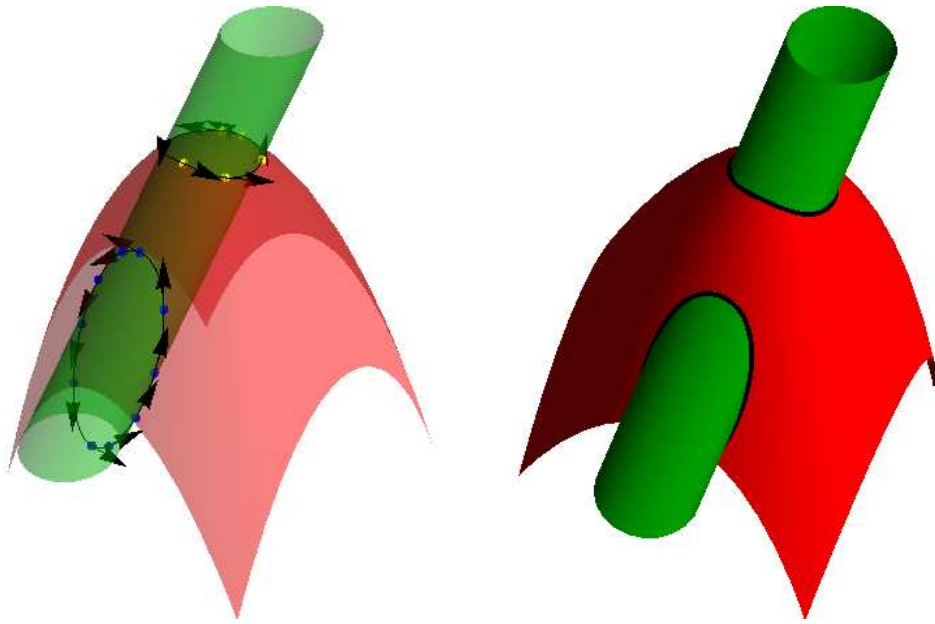
Figure 6.7: Sampled points and tangents in $\mathbb{R}^3$ (left), approximation of intersection by biarcs (right).

6.3 Joining canal surfaces

In this section we will show how to use biarcs when joining canal surfaces. A canal surface is a surface swept by a moving circle. The circle moves along the curve called spine and the radius of the circle can vary along the spine. We denote $\mathbf{s}(t)$ the parametric equation of the spine and $r(t)$ the function describing radius of circles. These circles lie in planes that are perpendicular to tangent vectors of the spine. To specify these planes we define the Frenet–Serret frame of the spine that consist of tangent, normal and binormal vectors

$$\mathbf{T}(t) = \frac{\mathbf{s'}(t)}{||\mathbf{s'}(t)||}, \tag{6.26}$$

$$\mathbf{N}(t) = \frac{\mathbf{T'}(t)}{||\mathbf{T'}(t)||}, \tag{6.27}$$

$$\mathbf{B}(t) = \mathbf{T}(t) \times \mathbf{N}(t), \tag{6.28}$$

where the dot symbolizes first derivative with respect to t. Circle forming the canal surface at a point $\mathbf{s}(t_0)$ lies in plane spanned by vectors $\mathbf{N}(t)$ and $\mathbf{B}(t)$ and containing the point $\mathbf{s}(t_0)$ (see Figure 6.8).

Canal surface is then described by parametric equation (c.f. [2])

$$\mathbf{c}(t, \alpha) = \mathbf{s}(t) + r(t)(\mathbf{N}(t) \cos \alpha + \mathbf{B}(t) \sin \alpha), \quad t \in (0, 1),\ \alpha \in (0, 2\pi). \tag{6.29}$$

We will now show how to construct a joining canal surface between two canal surfaces. Let us have canal surfaces $\mathbf{S}_1, \mathbf{S}_2$ defined by

$$\mathbf{s}_1(t), r_1(t) \quad t \in (0, 1), \tag{6.30}$$

and

$$\mathbf{s}_2(t), r_2(t) \quad t \in (0, 1), \tag{6.31}$$

with Frenet–Serret frames $(\mathbf{T}_1(t), \mathbf{N}_1(t), \mathbf{B}_1(t))$ and $(\mathbf{T}_2(t), \mathbf{N}_2(t), \mathbf{B}_2(t))$, respectively. First, we find the spine of the joining surface, which we construct as a biarc joining data pair $(\mathbf{P}_1, \mathbf{t}_1), (\mathbf{P}_2, \mathbf{t}_2)$, where

$$\mathbf{P}_1 = \mathbf{s}_1(1),\ \mathbf{P}_2 = \mathbf{s}_2(0),\,^2 \tag{6.32}$$

and

$$\mathbf{t}_1 = \mathbf{T}_1(1),\ \mathbf{t}_2 = \mathbf{T}_2(0). \tag{6.33}$$

---

[2]We can also set $\mathbf{P}_1 = \mathbf{s}_1(0)$ or $\mathbf{P}_2 = \mathbf{s}_2(1)$. It depends on the parts of surfaces we want to join.
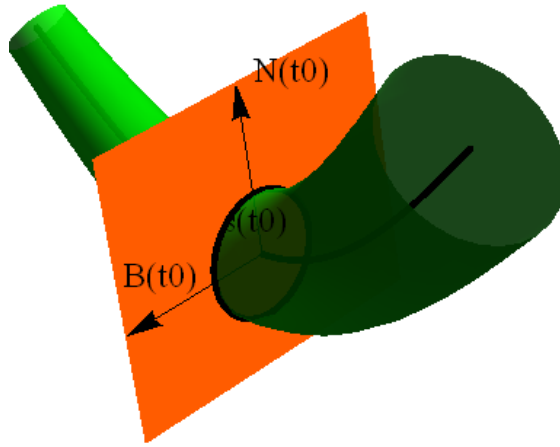
Figure 6.8: Plane spanned by vectors $\mathbf{N}(t)$ and $\mathbf{B}(t)$ and containing the point $\mathbf{s}(t_0)$.

Next we need to find function $r_3(t)$ that connects two radii functions $r_1(t), r_2(t)$. There are many ways how to do this, depending on the surface continuity we wish to preserve. Continuity of joined surfaces exceedes framework of this thesis. In our example, we have set $r_3(t)$ to be linear combination of $r_1(t), r_2(t)$

$$r_3(t) = (1 - t)r_1 + tr_2, \tag{6.34}$$

preserving only G^1 continuity of the spine curve. Figure 6.9 shows joining of two canal surfaces by the above method. The first canal surface is defined by

$$\begin{aligned} \mathbf{S}_1(t) &= (\pi t, \sin(\pi t), 0), \\ r_1(t) &= 0.1\pi t + 0.2, \quad t \in (0, 1) \end{aligned} \tag{6.35}$$

and the second canal surface by

$$\begin{aligned} \mathbf{S}_2(t) &= (5, 5t + 3, 0), \\ r_2(t) &= e^t, \quad t \in (0, 1). \end{aligned} \tag{6.36}$$

53

Figure 6.9: Two cannal surfaces joined by a cannal surface with biarc spine. Red canal surface is defined by (6.35). Green canal surface is defined by (6.36). Joining canal surface with biarc spine is shown in yellow.

Conclusion

In this thesis we have studied properties and applications of piecewise circular spline curves consisted of biarcs in plane and in space. We have presented theorem on how to choose the joining point to get biarc with G^1 continuity at this point. We have shown how to interpolate Hermitian data by biarcs by two techniques. Firstly by obvious technique - finding centres of circles, which gives simply described biarc but requires solving system of equations to get parameter values that form arc of circle. Secondly by rotating the chord vector, which does not require finding centres of arcs and parameter range, but results in more complicated description. We have also presented biarc construction by using NURBS formulation, that is very efficient description of biarc. Then we have discussed various choices of joining point and we have established construction of equal-chord and parallel-tangent biarc. We have also presented biarc that minimizes difference in curvatures of the two arcs. We have demonstrated how to approximate curve by piecewise circular spline when accuracy is given and we have shown that the order of approximation by equal-chord biarcs is three in plane as well as in space. Finally, we have presented some applications of piecewise circular spline curves in approximation of intersection of natural and rational surfaces and in joining cannal surfaces.

Some of the presented algorithms constructed in *Wolfram Mathematica 8* can be found on enclosed CD.

Bibliography

[1] Fix G., Hsu C.-P., Luo T., *Implicitization of rational parametric surfaces, J. Symbolic Computation, Vol.21, (1996), pp.329-336.*

[2] Garsia A., *Canal surfaces*(online), 2013-01[cit.2013-04-20], Available at World Wide Web ⟨*http://ieng9.ucsd.edu/ ma155f/classes/GOPHER.pdf*⟩.

[3] Kim T., Kim Y., Suh J.,· Zhang S., Yang Z., *Internal energy minimization in biarc interpolation, Advanced Manufacturing Technologies, Vol.44, (2009),pp.1165–1174.*

[4] Meek D. S., Walton D. J., *Approximating quadratic NURBS curves by arc splines, Computer-Aided Design, Vol.25, (1993), pp.371-376.*

[5] Meek D. S., Walton D. J., *Approximating smooth planar curves by arc splines, Journal of Computational and Applied Mathematics, Vol.59, (1995), pp.221-231.*

[6] Piegl L.A., Tiller W., *Biarc approximation of NURBS curves, Computer-Aided Design, Vol.34, (2002), pp.807-814.*

[7] Piegl L.A., Tiller W., *Data Approximation Using Biarcs, Engineering with Computers,Vol.18,(2002), pp.59-65.*

[8] Piegl L. A., Tiller W.,*The NURBS Book*, Springer-Verlag, 2nd ed. (1995–1997).

[9] Piegl L.A., Rajab K., Smarodzinava V., Valavanis K. P., *Using a biarc filter to compute curvature extremes of NURBS curves, Engineering with Computers, Vol.25, (2009), pp.379–387.*

[10] Rossignac J.R., Requicha A.A.G., *Piecewise circular curves for geometric modeling, IBM Journal of Research and Development, Vol.31, (1987), pp.296 - 313 .*

[11] Schönherr J., *Smooth biarc curves, Computer-Aided Design, Vol.25, (1993), pp.365-370.*

[12] Séquin C. H., Lee K, *Fair and Robust Circle Splines, Proceedings of the SIGGRAPH Conference on Sketches & Applications, (2003) .*

[13] SHARROCK T. J., *Surface Design with Cyclide Patches, PhD Thesis, University of Cambridge, Engineering Department, (1985).*

[14] SHEN L.-Y., CHENG J.-S., JIA X., *Homeomorphic approximation of the intersection curve of two rational surfaces, Computer Aided Geometric Design, Vol.29, (2012), pp.613-625.*

[15] SMUTNY J., *Global Radii of Curvature and the Biarc Approximation of Space Curves: In Pursuit of Ideal Knot Shapes*, PhD Thesis, l'Université de Zürich, (2004).

[16] ŠÍR, Z., FEICHTINGER, R., JÜTTLER, B., *Approximating Curves and Their Offsets using Biarcs and Pythagorean Hodograph Quintics, Computer-Aided Design, Vol. 38, (2006), pp. 608-618*

[17] YANG X., *Efficient circular arc interpolation based on active tolerance control, Computer-Aided Design, Vol.34, (2002), pp.1037-1046.*

All calculations and figures were created in software *Wolfram Mathematica* 8.